Table 1
The timing of the establishment of parental-origin-dependent differential methylation at secondary DMRs and imprinted expression of associated genes during post-zygotic development.

Imprinted gene	Secondary DMR	Methylation status established (methylated allele)	Monoallelic expression observed (expressed allele)	Primary DMR (methylated allele)	References
Gtl2	*Gtl2*-DMR	E6.5 (Pat)	Blastocyst (Mat)	IG-DMR (Pat)	This study
Cdkn1c	*Cdkn1c*-DMR	E9.5 (Pat)	Morula (Mat)	KvDMR1 (Mat)	[33,34]
Igf2	*Igf2*-DMR1/DMR2	E15.5 (Pat)	Blastocyst (Pat)	*H19*-DMR (Pat)	[13,35]
H19	*H19* promoter	E6.5 (Pat)	Morula (Mat)	*H19*-DMR (Pat)	[36]
Igf2r	*Igf2r*-DMR1	From E15.5 to 4dpp[a](Pat)	E6.5 (Mat)	*Igf2r*-DMR2 (Mat)	[37,38]

[a] Days post partum.

methylation at the paternal allele of the *Gtl2*-DMR. Assuming that the bivalent histone modification pattern observed at the MEG3/GTL2-DMR in human sperm is conserved in mice and is preserved in preimplantation embryos, our results can be explained by such histone modifications. If H3K27m3 and H3K4me3 marks are present at the paternal allele of the Gtl2-DMR in the blastocyst stage, these could be attributed to the paternal repression of Gtl2 and the absence of DNA methylation at the locus, respectively. Since the *Gtl2*-DMR was found to gain DNA methylation after the blastocyst stage, the H3K4me3 mark may be erased by then. It has been shown that in E12–14 embryos, the *Gtl2*-DMR is not enriched for the H3K27me3 mark on both parental alleles [45]. Therefore, the H3K27me3 mark may also be erased during or after the establishment of DNA methylation at the *Gtl2*-DMR. DNA methylation is considered to be more critical for the paternal repression of *Gtl2* in the absence of the H3K27me3 mark.

Our results demonstrate that during early post-zygotic development, the germline-derived DNA methylation on the paternal allele of the IG-DMR is partially lost by the E3.5 stage and its methylation is restored by E5.5. Histone modification patterns on the paternal allele of the IG-DMR may be responsible for the recruitment of de novo methylation machinery between E3.5 and E5.5 stages. In the human sperm, the IG-DMR is shown to be devoid of H3K4me3 [44]. If the non-methylated status of H3K4 is maintained on the paternal allele of the mouse IG-DMR at the blastocyst stage, the DNMT3L/DNMT3A complex may possibly be recruited to direct de novo cytosine methylation to restore the methylation of the IG-DMR.

We observed a reduction of DNA methylation levels on the paternal allele of the IG-DMR in blastocysts (E3.5) compared to methylation levels in the sperm. Loss of methylation on the paternal allele of IG-DMR was also observed in extra-embryonic tissues at the E7.5 stage compared to those at E5.5. Interestingly, throughout stages E3.5 to E7.5 of development, several CpG sites within the R1 region in the IG-DMR (such as 5th, 7th, 17th, 20th and 21st CpG sites in the R1 region in Fig. 1B–D and Supplementary Fig. 1) show high levels of DNA methylation on the paternal allele. These CpG sites may have greater functional importance than other CpGs in the IG-DMR. We also observed tissue-specific relaxation of differential methylation in the R2 and R3 regions of the IG-DMR among E15.5/16.5 tissues (Fig. 1C). It remains to be elucidated whether the R2 and R3 regions have critical roles in the regulation of imprinted expression in the *Dlk1-Dio3* cluster. Creation and characterization of a knockout mouse line with a mutation or a deletion at a particular subregion of IG-DMR will help further dissect the role of IG-DMR as the ICR of the *Dlk1-Dio3* cluster.

3.3. Difference in the allelic DNA methylation patterns between the embryonic and the extra-embryonic lineages at the Gtl2-DMR and the IG-DMR

Mechanisms that regulate the imprinted expression of maternally expressed ncRNAs in the *Dlk1-Dio3* domain are suggested to differ between the embryo and the placenta [21]. However, the principal mechanisms regulating allele-specific expression in each of the two lineages are unknown. The *Gtl2*-DMR was previously shown to be partially methylated on both parental alleles in the placenta of late gestation embryos (E16.5) [21]. Here, we clearly determined that the *Gtl2*-DMR is partially methylated on both parental alleles in the placenta as early as E6.5. Furthermore, our data demonstrated that part of the IG-DMR also becomes partially methylated on both parental alleles in the placenta by E7.5. Therefore, further epigenetic profiling of these DMRs in embryonic and extra-embryonic lineages, which include DNA methylation as well as histone modifications, will help define underlying regulatory mechanisms. The differential regulation of imprinted genes between the embryo and placenta has been well-characterized for the *Kcnq1* imprinted gene cluster [34,46,47]. In 2006, Lewis et al. subjected ES and TS cells as well as their differentiated derivates to epigenetic profiling [47]. These cells, which maintain imprinted expression of the *Kcnq1* cluster of genes, were found to establish monoallelic gene expression as well as differential histone marks for placenta-specific imprinted genes during differentiation of the extra-embryonic lineage between E4.5 and E7.5 [47]. The use of such stem cells would be an effective strategy to determine the epigenetic regulatory differences in the *Dlk1-Dio3* domain between the embryonic and the extra-embryonic lineages.

3.4. Developmental functions of genes within the Dlk1-Dio3 cluster

Gtl2 and *Dlk1* are shown to be expressed in most tissues after E12.5, and to reach their highest expression levels after E15.5 in several tissues [19]. In mice, maternally transmitted deletions of the IG-DMR or the *Gtl2*-DMR result in the dysregulation of imprinted expression of the genes within the *Dlk1-Dio3* cluster [15,21,23,24]. Such mice exhibit prenatal/perinatal lethality and dysplastic phenotypes in various tissues such as skeletal muscle, bone, liver, and lung [21,23,24]. Recently, iPSCs with repressed expression of maternally expressed ncRNAs within the *Dlk1-Dio3* cluster ($Gtl2^{off}$ iPSCs) were shown to contribute poorly to chimeras [25]. When $Gtl2^{off}$ and $Gtl2^{on}$ iPSCs were injected into tetraploid blastocysts, morphologically normal embryos (at E11.5) were obtained from both types of iPSCs. However, almost all embryos derived from the $Gtl2^{off}$ iPSCs were found to be dead at E11.5 [25]. These observations indicate that genes in the *Dlk1-Dio3* cluster play important roles in cell proliferation and/or differentiation, not only at late-gestation stages, but at developmental stages earlier than E11.5. In this study, we revealed that *Gtl2* is transiently up-regulated and expressed at comparably high levels at E5.5 to E6.5 stages. On the other hand, *Gtl2* is expressed at low levels in blastocysts and E7.5 to E11.5 embryos (this study and Ref. [19]). Taken together, *Gtl2* (and the other maternally expressed ncRNAs) may be involved in the control of proliferation and differentiation of cells at early gestation stages (E5.5 to E6.5).

4. Materials and methods

4.1. Sample preparations

To obtain early embryonic and extra-embryonic tissues, female C57BL/6 (B6) (*Mus musculus musculus*) mice (Sankyo Labo Service,

Tokyo, Japan) mated with male JF1/Ms (JF1) (*Mus musculus molossinus*) mice were sacrificed at appropriate stages according to the guidelines for the care and use of laboratory animals (National Research Institute for Child Health and Development, Japan). At noon on the day the copulation plug was found was designated as embryonic day 0.5 (E0.5). Three to six samples (whole embryos or dissected tissues) at each of the developmental stages from E3.5 to E6.5 were pooled. The numbers of the samples pooled were: six blastocysts (E3.5) for each of three independent pools (Blast _1 to Blast_3); four or five whole embryos at E5.5 for three independent pools (E5.5Emb_1 to E5.5Emb_3); three or four embryonic tissues at E6.5 for three independent pools (E6.5Emb_1 to E6.5Emb_3); three or four extra-embryonic tissues at E6.5 for three independent pools (E6.5Ex_1 to E6.5Ex_3). Embryonic and extra-embryonic tissues at E7.5 were prepared from three embryos and analyzed individually (E7.5Emb_1 to E7.5Emb_3, and E7.5Ex_1 to E7.5Ex_3). These pooled and individual samples were subjected to simultaneous isolation of genomic DNA and total RNA using Allprep DNA/RNA micro or mini kit (Qiagen, Hilden, Germany) according to the manufacturer's instructions. Fetal tissues (E16.5 skeletal muscle, E15.5 brain, and E16.5 liver) were obtained from the F1 hybrid fetuses derived from reciprocal matings between the B6 and the JF1 strains.

Spermatozoa were collected from the vas deferens of JF1 mice. Isolation of the DNA was performed as described previously [48]. Briefly, sperm genomic DNA was isolated by treatment with 1% 2-mercaptoethanol (Sigma-Aidrich, Tokyo, Japan) and proteinase K (Sigma), and followed by phenol/chloroform extraction and ethanol precipitation.

4.2. Sodium bisulfite genomic sequencing

Sodium bisulfite treatment was performed using EZ DNA methylation direct kit (Zymo Research, Orange, CA) according to the manufacturer's instructions. PCR was performed using one unit of Biotaq HS DNA polymerase (Bioline, London, UK) and primer sets as follows: 5′-TGTGTTGTGGATTTAGGTTGTAGTTTA-3′ and 5′-TAATCCCATTCCCAATCTATAAAAATA-3′ for R1 (nt 81187–81647), 5′-CCAAAACAAACCCAATAAATTCTAA-3′ and 5′-TGGTGAGTTTTGGTTAGAAAAGTGT-3′ for R2 (nt 82265–82615), 5′-CCCCCAATAACTTATAAACCATAATACT-3′ and 5′-GGATGGTAGTAGATAATTTGTTGTTTGA-3′ for R3 (nt 83273–83670), 5′-AAATCAAAATCCTTTTACCTCAACAATA-3′ and 5′-GGAAATAATTTTAATTGGTGATTGTTTT-3′ for R4 (nt 93435–93731), and 5′-AAATTTTGTAAGGAAAAGAATTTTTAGG-3′ and 5′-TTCAAAATTACTAATCAACATAAACCTC-3′ for R5 (nt 94288–94671). The thermocycling conditions were 35 to 45 cycles of 94 °C for 30 seconds (s), 55 °C for 30 s, and 72 °C for 30 s, with an initial step of 95 °C for 10 minutes (min) and a final step of 72 °C for 7 min. The amplified PCR products were cloned into pGEM T-Easy vector (Promega, Madison, WI), and sequenced by 3130xl Genetic Analyzer (Applied Biosystems, Foster city, CA). Nucleotide position (nt) and rs ID of SNPs and alleles (B6/JF1 alleles) within each region are as follows: R1, nt 81275 (rs46718958, A/G), nt 81422 (rs47741870, G/A), and nt 81610 (G/A); R2, nt 82369 (rs52043811, C/T); R3, nt 83406 (T/C), nt 83546 (rs46395233, C/T), nt 83593 (rs50881257, C/T), and nt 83631 (rs46982259, C/A); R4, nt 93671 (C/T); R5, nt 94561 (G/A). All nucleotide positions refer to the sequence of GenBank accession no. AJ320506.1. Allelic methylation patterns were assessed using two independent (pooled or individual) samples for the E3.5 to E7.5 stages, and using one each sample for the JF1 sperm and the E15.5/16.5 fetal tissues. The methylation patterns of individual clones are shown in Supplementary Fig. 1 for all regions and for all samples analyzed. Overall methylation percentage for each region (the number of methylated CpGs per number of total CpGs) was calculated for each type of tissues, and is shown in Fig. 1. When bisulfite sequencing data were available from two independent sample sets (for the tissues from the E3.5 to E7.5 stages), two datasets were combined to calculate the overall methylation percentage. The numbers of individual clones used to determine methylation percentages ranged from 5 to 35 (average 16.8).

4.3. Quantitative real-time RT-PCR

First strand cDNA synthesis was carried out by random hexamers using QuantiTect Reverse Transcription (Qiagen) according to the manufacturer's instructions. For quantitative real-time RT-PCR, amplification was performed using SYBR premix Ex taq (Takara, Kyoto, Japan) and primer sets as follows: 5′-CAGGACCCTCCAACTGTAAATC-3′ and 5′-AGGTAGGAACCTGAGCCCATTT-3′ for *Gtl2* (nt 1553–1818); 5′-CTCTTGCTCCTGCTGGCTTT-3′ and 5′-CTTGTGCTGGCAGTCCTTTC-3′ for *Dlk1* (nt 176–526); 5′-CTGCACCACCAACTGCTTAG-3′ and 5′-CCTGCTTCACCACCTTCTTG-3′ for *Gapdh*. Ct values for *Dlk1* and *Gtl2* as well as *Gapdh* as a reference were determined using the 7900HT fast real-time PCR system (Applied Biosystems). The average Ct value was calculated from the Ct values from duplicate reactions for the same cDNA sample. The relative expression levels of *Dlk1* and *Gtl2* were determined by the delta–delta Ct method. Delta Ct values were calculated using the Ct values of *Gapdh* as a reference gene. Delta–delta Ct values were calculated using the average delta Ct value of E16.5 skeletal muscle samples as a reference. To determine the range of Ct values in which quantitative accuracy is expected for *Dlk1*, *Gtl2*, and *Gapdh*, we generated a standard curve for each of the genes using an 8-fold dilution series (six dilutions) of a cDNA sample (12.5 dpc placenta). We obtained a linear standard curve showing $R^2 > 0.999$ with the Ct value ranging from 21.6 to 36.8 (amplification efficiency per cycle = 97.1%) for *Dlk1*, from 20.0 to 35.3 (95.6%) for *Gtl2*, and from 16.0 to 28.3 (95.9%) for *Gapdh*.

4.4. Allelic expression analysis by pyrosequencing

RT-PCR was performed using one unit of Biotaq HS DNA polymerase. The thermocycling conditions were 35 to 45 cycles of 94 °C for 30 s, 55 °C for 30 s, and 72 °C for 30 s, with an initial step of 95 °C for 10 min and a final step of 72 °C for 7 min. The primer sets used (and PCR product size in parentheses) are 5′-biotin-CAGGACCCTCCAACTGTAAATC-3′ and 5′-AGGTAGGAACCTGAGCCCATTT-3′ for *Gtl2* (266 bp), and 5′-CTCTTGCTCCTGCTGGCTTT-3′ and 5′-biotin-CTTGTGCTGGCAGTCCTTTC-3′ for *Dlk1* (94 bp). Pyrosequencing was carried out using the PSQ 96 MA system (Qiagen) and the PSQ 96 SNP Reagent kit (Qiagen) according to the manufacturer's instructions. In brief, the biotinylated PCR products were purified with the Streptavidin Sepharose HP beads (GE Healthcare, Uppsala, Sweden). The purified PCR products were washed, denatured and then annealed with a sequencing primer (5′-GGCGTCCCCGTGGCT-3′ for *Gtl2* and 5′-ATGCGACCCACCCTG-3′ for *Dlk1*). The nucleotide position and alleles (B6/JF1) of SNPs within the regions analyzed are nt 1579 of NR_027652.1 (rs46969056; A/G on the reverse strand) for *Gtl2* and nt 235 of NM_010052.4 (T/C on the forward strand) for *Dlk1*.

Supplementary materials related to this article can be found online at doi:10.1016/j.ygeno.2011.05.003.

Acknowledgments

We thank Dr. Layla Parker-Katiraee for her critical reading of the manuscript. This study was supported by Grants-in-Aid for Scientific Research on Priority Areas from the Ministry of Education, Culture, Sports, Science and Technology, Japan, to KH and KN, and by and a Grant-in Aid for Scientific Research from the Japan Society for the Promotion of the Science to KN.

References

[1] A.C. Ferguson-Smith, M.A. Surani, Imprinting and the epigenetic asymmetry between parental genomes, Science 293 (2001) 1086–1089.
[2] D. Lucifero, M.R. Mann, M.S. Bartolomei, J.M. Trasler, Gene-specific timing and epigenetic memory in oocyte imprinting, Hum. Mol. Genet. 13 (2004) 839–849.

[3] H. Hiura, Y. Obata, J. Komiyama, M. Shirai, T. Kono, Oocyte growth-dependent progression of maternal imprinting in mice, Genes Cells 11 (2006) 353–361.
[4] T.L. Davis, J.M. Trasler, S.B. Moss, G.J. Yang, M.S. Bartolomei, Acquisition of the *H19* methylation imprint occurs differentially on the parental alleles during spermatogenesis, Genomics 58 (1999) 18–28.
[5] J.Y. Li, D.J. Lees-Murdock, G.L. Xu, C.P. Walsh, Timing of establishment of paternal methylation imprints in the mouse, Genomics 84 (2004) 952–960.
[6] H. Hiura, J. Komiyama, M. Shirai, Y. Obata, H. Ogawa, T. Kono, DNA methylation imprints on the IG-DMR of the *Dlk1-Gtl2* domain in mouse male germline, FEBS Lett. 581 (2007) 1255–1260.
[7] D. Bourc'his, G.L. Xu, C.S. Lin, B. Bollman, T.H. Bestor, Dnmt3L and the establishment of maternal genomic imprints, Science 294 (2001) 2536–2539.
[8] K. Hata, M. Okano, H. Lei, E. Li, Dnmt3L cooperates with the Dnmt3 family of de novo DNA methyltransferases to establish maternal imprints in mice, Development 129 (2002) 1983–1993.
[9] M. Kaneda, M. Okano, K. Hata, T. Sado, N. Tsujimoto, E. Li, H. Sasaki, Essential role for *de novo* DNA methyltransferase Dnmt3a in paternal and maternal imprinting, Nature 429 (2004) 900–903.
[10] Y. Kato, M. Kaneda, K. Hata, K. Kumaki, M. Hisano, Y. Kohara, M. Okano, E. Li, M. Nozaki, H. Sasaki, Role of the Dnmt3 family in de novo methylation of imprinted and repetitive sequences during male germ cell development in the mouse, Hum. Mol. Genet. 16 (2007) 2272–2280.
[11] S.K. Ooi, C. Qiu, E. Bernstein, K. Li, D. Jia, Z. Yang, H. Erdjument-Bromage, P. Tempst, S.P. Lin, C.D. Allis, X. Cheng, T.H. Bestor, DNMT3L connects unmethylated lysine 4 of histone H3 to de novo methylation of DNA, Nature 448 (2007) 714–717.
[12] D. Jia, R.Z. Jurkowska, X. Zhang, A. Jeltsch, X. Cheng, Structure of Dnmt3a bound to Dnmt3L suggests a model for de novo DNA methylation, Nature 449 (2007) 248–251.
[13] S. Lopes, A. Lewis, P. Hajkova, W. Dean, J. Oswald, T. Forne, A. Murrell, M. Constancia, M. Bartolomei, J. Walter, W. Reik, Epigenetic modifications in an imprinting cluster are controlled by a hierarchy of DMRs suggesting long-range chromatin interactions, Hum. Mol. Genet. 12 (2003) 295–305.
[14] J.Y. Shin, G.V. Fitzpatrick, M.J. Higgins, Two distinct mechanisms of silencing by the KvDMR1 imprinting control region, EMBO J. 27 (2008) 168–178.
[15] S.P. Lin, N. Youngson, S. Takada, H. Seitz, W. Reik, M. Paulsen, J. Cavaille, A.C. Ferguson-Smith, Asymmetric regulation of imprinting on the maternal and paternal chromosomes at the *Dlk1-Gtl2* imprinted cluster on mouse chromosome 12, Nat. Genet. 35 (2003) 97–102.
[16] P. Szabó, S.H. Tang, A. Rentsendorj, G.P. Pfeifer, J.R. Mann, Maternal-specific footprints at putative CTCF sites in the *H19* imprinting control region give evidence for insulator function, Curr. Biol. 10 (2000) 607–610.
[17] F. Sleutels, R. Zwart, D.P. Barlow, The non-coding *Air* RNA is required for silencing autosomal imprinted genes, Nature 415 (2002) 810–813.
[18] D. Mancini-Dinardo, S.J. Steele, J.M. Levorse, R.S. Ingram, S.M. Tilghman, Elongation of the *Kcnq1ot1* transcript is required for genomic imprinting of neighboring genes, Genes Dev. 20 (2006) 1268–1282.
[19] S. Takada, M. Tevendale, J. Baker, P. Georgiades, E. Campbell, T. Freeman, M.H. Johnson, M. Paulsen, A.C. Ferguson-Smith, *Delta-like* and *Gtl2* are reciprocally expressed, differentially methylated linked imprinted genes on mouse chromosome 12, Curr. Biol. 10 (2000) 1135–1138.
[20] S. Takada, M. Paulsen, M. Tevendale, C.E. Tsai, G. Kelsey, B.M. Cattanach, A.C. Ferguson-Smith, Epigenetic analysis of the *Dlk1-Gtl2* imprinted domain on mouse chromosome 12: implications for imprinting control from comparison with *Igf2-H19*, Hum. Mol. Genet. 11 (2002) 77–86.
[21] S.P. Lin, P. Coan, S.T. da Rocha, H. Seitz, J. Cavaille, P.W. Teng, S. Takada, A.C. Ferguson-Smith, Differential regulation of imprinting in the murine embryo and placenta by the *Dlk1-Dio3* imprinting control region, Development 134 (2007) 417–426.
[22] M. Kagami, M.J. O'Sullivan, A.J. Green, Y. Watabe, O. Arisaka, N. Masawa, K. Matsuoka, M. Fukami, K. Matsubara, F. Kato, A.C. Ferguson-Smith, T. Ogata, The IG-DMR and the *MEG3*-DMR at human chromosome 14q32.2: hierarchical interaction and distinct functional properties as imprinting control centers, PLoS Genet. 6 (2010) e1000992.
[23] N. Takahashi, A. Okamoto, R. Kobayashi, M. Shirai, Y. Obata, H. Ogawa, Y. Sotomaru, T. Kono, Deletion of *Gtl2*, imprinted non-coding RNA, with its differentially methylated region induces lethal parent-origin-dependent defects in mice, Hum. Mol. Genet. 18 (2009) 1879–1888.
[24] Y. Zhou, P. Cheunsuchon, Y. Nakayama, M.W. Lawlor, Y. Zhong, K.A. Rice, L. Zhang, X. Zhang, F.E. Gordon, H.G. Lidov, R.T. Bronson, A. Klibanski, Activation of paternally expressed genes and perinatal death caused by deletion of the *Gtl2* gene, Development 137 (2010) 2643–2652.
[25] M. Stadtfeld, E. Apostolou, H. Akutsu, A. Fukuda, P. Follett, S. Natesan, T. Kono, T. Shioda, K. Hochedlinger, Aberrant silencing of imprinted genes on chromosome 12qF1 in mouse induced pluripotent stem cells, Nature 465 (2010) 175–181.
[26] H. Kobayashi, C. Suda, T. Abe, Y. Kohara, T. Ikemura, H. Sasaki, Bisulfite sequencing and dinucleotide content analysis of 15 imprinted mouse differentially methylated regions (DMRs): paternally methylated DMRs contain less CpGs than maternally methylated DMRs, Cytogenet Genome Res. 113 (2006) 130–137.
[27] W. Reik, W. Dean, J. Walter, Epigenetic reprogramming in mammalian development, Science 10 (2001) 1089–1093.
[28] H.D. Morgan, F. Santos, K. Green, W. Dean, W. Reik, Epigenetic reprogramming in mammals, Hum. Mol. Genet. 14 (2005) R47–R58.
[29] J.V. Schmidt, P.G. Matteson, B.K. Jones, X.J. Guan, S.M. Tilghman, The *Dlk1* and *Gtl2* genes are linked and reciprocally imprinted, Genes Dev. 14 (2000) 1997–2002.
[30] M. Kagami, Y. Sekita, G. Nishimura, M. Irie, F. Kato, M. Okada, S. Yamamori, H. Kishimoto, M. Nakayama, Y. Tanaka, K. Matsuoka, T. Takahashi, M. Noguchi, Y. Tanaka, K. Masumoto, T. Utsunomiya, H. Kouzan, Y. Komatsu, H. Ohashi, K. Kurosawa, K. Kosaki, A.C. Ferguson-Smith, F. Ishino, T. Ogata, Deletions and epimutations affecting the human 14q32.2 imprinted region in individuals with paternal and maternal upd(14)-like phenotypes, Nat. Genet. 40 (2008) 237–242.
[31] K. Schuster-Gossler, P. Bilinski, T. Sado, A. Ferguson-Smith, A. Gossler, The mouse *Gtl2* gene is differentially expressed during embryonic development, encodes multiple alternatively spliced transcripts, and may act as an RNA, Dev. Dyn. 212 (1998) 214–228.
[32] S.T. da Rocha, M. Tevendale, E. Knowles, S. Takada, M. Watkins, A.C. Ferguson-Smith, Restricted co-expression of Dlk1 and the reciprocally imprinted non-coding RNA, Gtl2: implications for cis-acting control, Dev. Biol. 306 (2007) 810–823.
[33] B. Bhogal, A. Arnaudo, A. Dymkowski, A. Best, T.L. Davis, Methylation at mouse *Cdkn1c* is acquired during postimplantation development and functions to maintain imprinted expression, Genomics 84 (2004) 961–970.
[34] D. Umlauf, Y. Goto, R. Cao, F. Cerqueira, A. Wagschal, Y. Zhang, R. Feil, Imprinting along the *Kcnq1* domain on mouse chromosome 7 involves repressive histone methylation and recruitment of Polycomb group complexes, Nat. Genet. 36 (2004) 1296–1300.
[35] M. Ohno, N. Aoki, H. Sasaki, Allele-specific detection of nascent transcripts by fluorescence in situ hybridization reveals temporal and culture-induced changes in *Igf2* imprinting during pre-implantation mouse development, Genes Cells 6 (2001) 249–259.
[36] H. Sasaki, A.C. Ferguson-Smith, A.S. Shum, S.C. Barton, M.A. Surani, Temporal and spatial regulation of *H19* imprinting in normal and uniparental mouse embryos, Development 121 (1995) 4195–4202.
[37] R. Stöger, P. Kubicka, C.G. Liu, T. Kafri, A. Razin, H. Cedar, D.P. Barlow, Maternal-specific methylation of the imprinted mouse *Igf2r* locus identifies the expressed locus as carrying the imprinting signal, Cell 73 (1993) 61–71.
[38] W. Lerchner, D.P. Barlow, Paternal repression of the imprinted mouse *Igf2r* locus occurs during implantation and is stable in all tissues of the post-implantation mouse embryo, Mech. Dev. 61 (1997) 141–149.
[39] Y. Sekita, H. Wagatsuma, M. Irie, S. Kobayashi, T. Kohda, J. Matsuda, M. Yokoyama, A. Ogura, K. Schuster-Gossler, A. Gossler, F. Ishino, T. Kaneko-Ishino, Aberrant regulation of imprinted gene expression in *Gtl2*^{lacZ} mice, Cytogenet Genome Res. 113 (2006) 223–229.
[40] E.Y. Steshina, M.S. Carr, E.A. Glick, A. Yevtodiyenko, O.K. Appelbe, J.V. Schmidt, Loss of imprinting at the *Dlk1-Gtl2* locus caused by insertional mutagenesis in the *Gtl2* 5′ region, BMC Genet. 7 (2006) 44.
[41] T. Fan, J.P. Hagan, S.V. Kozlov, C.L. Stewart, K. Muegge, Lsh controls silencing of the imprinted *Cdkn1c* gene, Development 132 (2005) 635–644.
[42] J. Mager, N.D. Montgomery, F.P. de Villena, T. Magnuson, Genome imprinting regulated by the mouse Polycomb group protein Eed, Nat. Genet. 33 (2003) 502–507.
[43] R. Margueron, N. Justin, K. Ohno, M.L. Sharpe, J. Son, W.J. Drury III, P. Voigt, S.R. Martin, W.R. Taylor, V. De Marco, V. Pirrotta, D. Reinberg, S.J. Gamblin, Role of the Polycomb protein EED in the propagation of repressive histone marks, Nature 461 (2009) 762–767.
[44] S.S. Hammoud, D.A. Nix, H. Zhang, J. Purwar, D.T. Carrell, B.R. Cairns, Distinctive chromatin in human sperm packages genes for embryo development, Nature 460 (2009) 473–478.
[45] M.S. Carr, A. Yevtodiyenko, C.L. Schmidt, J.V. Schmidt, Allele-specific histone modifications regulate expression of the *Dlk1-Gtl2* imprinted domain, Genomics 89 (2007) 280–290.
[46] A. Lewis, K. Mitsuya, D. Umlauf, P. Smith, W. Dean, J. Walter, M. Higgins, R. Feil, W. Reik, Imprinting on distal chromosome 7 in the placenta involves repressive histone methylation independent of DNA methylation, Nat. Genet. 36 (2004) 1291–1295.
[47] A. Lewis, K. Green, C. Dawson, L. Redrup, K.D. Huynh, J.T. Lee, M. Hemberger, W. Reik, Epigenetic dynamics of the *Kcnq1* imprinted domain in the early embryo, Development 133 (2006) 4203–4210.
[48] M. Ariel, J. McCarrey, H. Cedar, Methylation patterns of testis-specific genes, Proc. Natl. Acad. Sci. U S A 88 (1991) 2317–2321.

Neoplastic transformation by TERT in FGF-2-expanded human mesenchymal stem cells

EMI YAMAOKA[1,2], EISO HIYAMA[1,2], YUSUKE SOTOMARU[1], YOSHIYUKI ONITAKE[2], IKUKO FUKUBA[2], TAKESHI SUDO[2], TAIJIRO SUEDA[2] and KEIKO HIYAMA[1]

[1]Natural Science Center for Basic Research and Development, [2]Department of Surgery, Graduate School of Biomedical Science, Hiroshima University, Hiroshima, Japan

Received January 28, 2011; Accepted April 4, 2011

DOI: 10.3892/ijo.2011.1029

Abstract. The low percentage of human mesenchymal stem cells (hMSCs) in bone marrow necessitates their *in vitro* expansion prior to clinical use in regenerative medicine. We evaluated the effect of long-term culture of hMSCs on telomere length and transformation capacity by TERT transfection. hMSCs were isolated from the bone marrow aspirates of 24 donors and cultured with fibroblast growth factor-2 (FGF-2). Six cell lines with >500 population doubling levels were considered immortalized. TERT was transfected into two of the six lines for a comparison of telomere length, telomerase activity, differential capacity, colony formation capacity in soft agar and tumorigenicity in immunodeficient (NOD-SCID) mice. hMSC lines exhibited elongated telomeres without the activation of telomerase and retained multi-lineage differentiation potential upon chondrogenic or adipogenic differentiation, while non-immortalized hMSCs showed a marked reduction in telomere length in the differentiation process. Immortalized hMSCs showed anchorage-independence and formed tumors in NOD-SCID mice. Histologically, these tumors consisted of differentiated cells such as fat tissue and cartilage. Two TERT-transfected hMSC lines showed high rates of tumor formation in NOD-SCID mice. These tumors were histologically similar to teratocarcinoma without differentiated cells. These cells may provide a model for the origin of cancer stem cells from adult stem cells, and indicate the possibility that telomerase activation has a major role in the malignant transformation of human stem cells. These data suggest that adult hMSCs have a potential for neoplastic transformation and have implications for the use of hMSCs in tissue engineering and regenerative medicine.

Introduction

Stem cells in various adult tissues play an important role in the regeneration of damaged tissue and maintenance of homeostasis in the tissues in which they reside. Human mesenchymal stem cells (hMSCs) are of great interest in regenerative medicine because they have the potential to differentiate into a variety of cells such as osteoblasts, adipocytes, chondrocytes, myocytes, and probably neuronal cells (1-5). Because of these properties, hMSCs might be a potential resource for future cell therapy. The goal of this study is to establish clinical cell lines with long life spans that retain their parental properties. However, clinical application has been difficult due to problems with retaining enhanced viability during storage, isolating cell populations with specific criteria, and expanding an *in vitro* system to obtain a sufficient number of cells without affecting their genomic characteristics and differentiation properties.

At present, there is very little evidence of whether changes in these properties occur during expansion. Normal hMSCs have a limited replicative capacity of at most 40- to 50-population doubling levels (PDL). The clinical use of hMSCs requires a large number of cells. Fibroblast growth factor-2 (FGF-2) increases PDL in hMSC monolayer cultures while preserving the differentiation potential (6,7). These FGF-2 expanded MSCs [FGF(+) hMSCs] exhibited long telomeres without upregulation of telomerase activity. Then, to elucidate the function of telomerase in hMSCs, we transfected TERT in these FGF(+) hMSC cell lines. In this study, we report on the immortalization of hMSCs by ALT (alternative lengthening of telomeres) and the neoplastic activity of these immortalized hMSCs following TERT transfection. The results indicate that immortalization might be regulated by ALT and that telomerase activation might be correlated with malignant transformation in hMSCs.

Materials and methods

Cell lines and TERT transfection. Human mesenchymal stem cells were isolated from bone marrow (BM) aspirates of 24 human donors (16 men and 8 women, from 16 to 64 years of age) after obtaining informed consent as previously described (7). Aspirates were cultured in high-glucose Dulbecco's modified Eagle's medium (DMEM, Invitrogen Corp., Carlsbad, CA, USA) containing 15% heat-inactivated FBS (Sigma-Aldrich, St. Louis, MO, USA) and antimicrobial agents. After confirming cell adhesion, hMSCs were cultured with or without FGF-2 (final

Correspondence to: Dr Eiso Hiyama, Hiroshima University, 1-2-3 Kasumi, Minami-ku, Hiroshima 734-8551, Japan
E-mail: eiso@hiroshima-u.ac.jp

Key words: stem cell, telomerase, TERT, immortality, cancer

concentration 1 ng/ml; R&D Systems Inc., Minneapolis, MN, USA). After again reaching confluence, the cells were reseeded under the same conditions. Six samples proliferated for >500 PDL. These cells were transfected with the TERT expression plasmid hTERTn2 (provided by Professor F. Ishikawa). hMSCs were transfected by using TransIT®-LT1 Reagent (Mirus Bio Corp., Madison, WI, USA) with 2 μg of hTERTn2 linearized with *Nru*I or with the vector plasmid linearized. G418 (Wako, Osaka, Japan) (300 μg/ml) was added to the medium after 24 h to select for clones harboring the transfected gene. G418 selection was continued for at least 1 month in exponentially growing cultures. hMSCs and TERT-transfected hMSCs were collected at various PDLs using trypsin followed by a rinse with PBS and were stored at -80°C.

Telomere length analysis. Telomere length was estimated using the length of terminal restriction fragments (TRFs) as measured by Southern blot analysis (8,9). Genomic DNA was isolated using proteinase K followed by phenol/chloroform extraction. Extracted DNA was completely digested with *Hin*fI, electrophoresed in a 0.6% agarose gel (2 μg/lane), transferred to a nitrocellulose membrane, and hybridized with 5'-end [^{32}P]-labeled $(TTAGGG)_4$. The length of the peak signals measured by the Bioimage Analyzer, BAS-2000 (Fuji film, Kanagawa, Japan) was estimated as the length of TRFs. Digested DNA was also subjected to pulse-field gel electrophoresis for the evaluation of long TRFs.

Telomere length was also measured by a fluorescence *in situ* hybridization (FISH) technique known as TeloFISH. TeloFISH was performed using a fluorescein isothiocyanate (FITC)-labeled peptide nucleic acid (PNA) probe specific for (TTAGGG)*n* sequences (Telomere PNA FISH Kit/FITC, Dako Cytomation Co., Kyoto, Japan). Briefly, hMSCs were treated with colcemid (10 μg/ml, Life Technologies) to prepare metaphase spreads and were pre-fixed with 2 ml freshly made fixative (3+1 v/v methanol/glacial acetic acid). After 10 min at room temperature, cells were centrifuged at 500 x g for 10 min. This pre-fix treatment was performed three times. The fixed cells were fixed to the slides, denatured at 80°C for 3 min, and hybridized with the FITC-conjugated telomere PNA probe for 30 min. The slides were then rinsed and washed at 65°C for 5 min and counterstained with DAPI.

Assay for telomerase activity and detection for TERT. Extraction of telomerase protein and evaluation of its activity were performed using the telomeric repeat amplification protocol (TRAP) (10,11). Briefly, 10^5-10^6 cells were homogenized in CHAPS lysis buffer. After 30 min of incubation on ice, the levels of telomerase activity were measured using the TRAPeze XL Kit (Serological Co., Gaithersburg, MD, USA), which is a quantitative, fluorescently-labeled PCR system for the estimation of relative telomerase activity levels with the use of a PCR internal control. The levels of fluorescein and sulforhodamine in each PCR product were measured in a fluorescent plate reader (Wallac, Perkin-Elmer, Wellesley, MA, USA). The level of telomerase activity, expressed in units of total product generated (TPG), was quantified by the ratio of the fluorescein intensity of the entire TRAP ladder in each sample (which was corrected with respect to the negative control) to the sulforhodamine intensity of the internal control (which was corrected with respect to background).

The expression levels of TERT in hMSCs were estimated by the reverse transcription-quantitative polymerase chain reaction. Total cellular RNA was extracted from tumor tissues by acid-guanidium-phenol chloroform method (12). First strand complementary DNA (cDNA) was synthesized with reverse transcriptase and random primers using a High-Capacity cDNA Archive Kit (Applied Biosystems, Foster City, CA). An aliquot of the cDNA (equivalent to 20 ng total RNA) was subjected to real-time RT-PCR using the TaqMan Gene Expression Assay (Applied Biosystems) for *TERT* and Pre-Developed TaqMan Assay Reagents (Applied Biosystems) for *18S* as an internal control. Results of the three or more independent measurements were averaged, and the relative gene expression levels were calculated as ratios to *18S* expression levels for each sample.

Induction of chondrogenic, adipogenic, and osteogenic differentiation. Chondrogenic adipogenic and osteogenic differentiation potential were measured in hMSCs and TERT-transfected hMSCs. A modified version of Johnstone's pellet culture system was used to induce chondrogenesis. Cells (10^6) were placed in a 15-ml polypropylene tube (Greiner BioOne, Frickenhausen, Germany) and centrifuged. The pellet was cultured at 37°C in a humidified atmosphere of 95% air and 5% CO_2 in 1 ml of chondrogenic medium containing high-glucose DMEM (Invitrogen) supplemented with 10 ng/ml transforming growth factor (TGF)-β3 (Sigma), 10^{-7} M dexamethasone (Sigma), 50 μg/ml ascorbic acid-2-phosphate sesquimagnesium salt (Sigma), 40 μg/ml L-proline (Nacalai tesque, Kyoto, Japan), ITS-A supplement (Invitrogen; 10 μg/ml insulin, 6.7 ng/ml sodium selenite, 5.5 μg/ml transferrin, 110 μg/ml sodium pyruvate), and 1.25 mg/ml bovine serum albumin (BSA, Sigma). Adipogenic differentiation was assessed by incubating cells with Adipogenic Induction Medium (Cambrex Bio Sciences, Walkersville, MD, USA) and maintained in hMSC Adipogenic Maintenance SingleQuots (Cambrex Bio Sciences) for 2-3 weeks. Adipocytes are recognized by the accumulation of lipid-containing vacuoles that stain red with Oil Red-O. Osteogenic differentiation was assessed by incubating the cells with DMEM-LG and 10% FBS supplemented with 0.1 μM dexamethasone, 10 μM β-glycerophosphate, and 50 μM ascorbate (all from Sigma-Aldrich) for 2-3 weeks. Cultures were stained with silver nitrate (von Kossa's staining) to assess mineralization.

Colony formation assay with soft agar. Anchorage-dependency of the cells was evaluated by conventional colony formation assay with soft agar. Trypsinized cells ($5x10^3$) were resuspended in DMEM containing 10% FBS and 0.4% SeaPlaque GTG agarose (Bio-products) and poured onto bottom ager containing 10% FBS and 0.53% agarose in a 30-mm culture dish. After 21 days of culture at 37°C with 5% CO_2, colony number was evaluated with crystal violet staining.

Transplantation of hMSCs in immunocompromised non-obese diabetic (NOD)-SCID mice. Tumor cells were resuspended in a 1:1 mixture of Matrigel (Becton-Dickinson) and serum-free medium (DMEM with 1% penicillin/streptomycin). A 100-μl

suspension containing between 100 and 100000 cells was injected subcutaneously (s.c.) into the flanks of 6- to 10-week-old male NOD/SCID immunodeficient mice obtained from CLEA Japan (Tokyo, Japan). If tumors developed, tumor cells were dispersed and subcutaneously injected into second-recipient NOD-SCID mice. Animal studies were approved by the Institutional Animal Care and Use Committee (Hiroshima University IRB No. A06-43) and conducted according to the Institutional Guidelines of Hiroshima University.

A portion of each developed tumor was re-cultured *in vitro* under the same conditions as the original tumor cells. The remainder of the tumor was fixed in formalin for pathological examination. The expression of TERT was detected by immunohistochemistry using an affinity-purified polyclonal rabbit antibody against TERT (EST21A) (Alpha Diagnostic International, San Antonio, TX) as previously described (13).

Statistical analysis. The data are shown as the mean ± SEM. Fisher's exact test was used for 2x2 contingency tables.

Results

Culture of hMSCs. Since hMSCs cultured without FGF-2 [MSCs-FGF(-)] entered senescence after approximately 20 PDLs, these hMSCs were cultured with FGF-2 [MSCs-FGF(+): FGF-2-expanded hMSCs]. FGF-2 was added to the culture at a final concentration of 1 ng/ml; these cells achieved more than 100 PDLs, doubling four times over a 4-day period, and exhibited small spindle-shaped aspects (Fig. 1A). It was these small spindle-shaped cells that had a high proliferation potential (Fig. 1B). Among 24 hMSC clones cultured with FGF-2, 6 had high proliferative activity (>100 PDLs). These clones have approximately the same proliferative rate in DMEM with or without FGF-2, and were considered to be immortalized hMSC clones (Fig. 1C).

TERT or vector alone was transfected into these 6 clones after 100 PDL. These cells, which were obtained after selection with 300 μg/ml of G418, were similar to pre-transfection cells in proliferative activity and morphology. The cell lines proliferated indefinitely (>1000 PDL) without major morphological changes after transfection with TERT (Fig. 1B and C). These cell lines were used in all subsequent analyses.

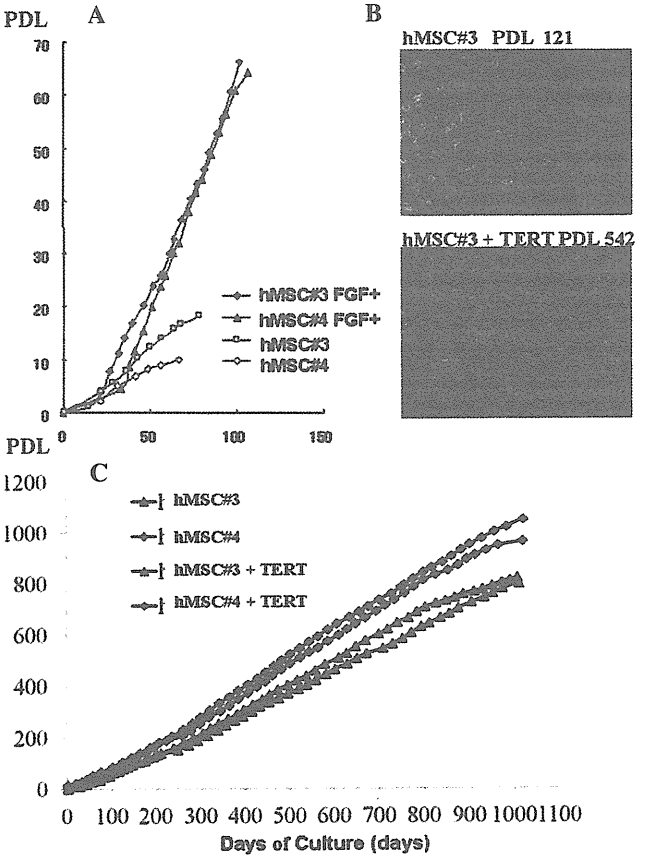

Figure 1. Cell proliferation and morphology of hMSCs. (A), Proliferation curve of FGF(+) hMSC or FGF(-) hMSC derived from bone marrow aspirates of normal human donors aged 32 (hMSC#3), and 43 years (hMSC#4) of age, respectively. After confirming cell adhesion to the plate, MSCs were cultured with 15% FBS-DMEM with or without FGF-2 (final concentration 1 ng/ml). Cumulative population doublings level (PDL) is regarded as zero for culture starting immediately after the primary culture of cells, and calculated to increase according to the equation: $\log_2$ {(the number of collected cells)/(the number of seeded cells)}. After TERT was transfected into FGF(+) hMSCs after culture of the 100 PDL. (B), Representative morphologies of hMSC (hMSC#3 PDL 121) and TERT-transfected hMSC (hMSC#3 + TERT PDL 542). There are no morphological changes after TERT transfection. (C), Proliferation curve of hMSCs or TERT transfected hMSCs of 2 clones (hMSC#3 and hMSC#4). Cumulative PDL is zero immediately after the primary culture of cells, and is calculated according to the equation: $\log_2$ {(the number of collected cells)/(the number of seeded cells)}. There are no changes of proliferative activity after TERT transfection.

Telomere length and telomerase in hMSCs and TERT-transfected hMSCs. Southern blot analysis showed that immortalized hMSCs maintain relatively long telomeric lengths (>23 kb). Pulse-field electrophoresis confirmed that the length of these elongated telomeres was approximately 40 kb (Fig. 2A). TeloFISH analysis also detected long telomeres in these expanded hMSCs and TERT-transfected hMSCs (Fig. 2B). However, there was no detectable telomerase activity in these hMSCs. Therefore, these findings suggest that long telomeres in hMSCs are maintained by a telomerase-independent mechanism.

Telomere lengths in TERT-transfected hMSCs were similar to those in untransfected hMSCs. The TRAP assay detected telomerase activity in TERT-transfected hMSCs but none in vector-transfected cells. All six lines showed high telomerase activity (14.6-1349.2 TPG) at 1-month post-transfection. The six TERT-transfected hMSC clones were cultured for more than 100 PDLs before telomerase activity was measured again. Telomerase activity was diminished in four clones (0.2-1.31 TPG in hMSC lines #1, #2, #5, and #6) and retained in two (1761.3 and 965.3 TPG in hMSC lines #3 and #4, respectively). TERT expression was also detected in these 6 clones just after transfection using RT-PCR, but retained in only two clones (hMSC#3 and hMSC#4) (Fig. 3). Among these 6 cell lines, we focused on the two clones with retained telomerase and TERT expression for the following examination.

In vitro differentiation potential in lineages of immortalized hMSC lines. hMSCs reportedly have an extensive potential to differentiate into multiple cell lineages including osteoblasts, chondrocytes, and adipocytes (14). To evaluate the effect of TERT transfection on differentiation, each hMSC line was

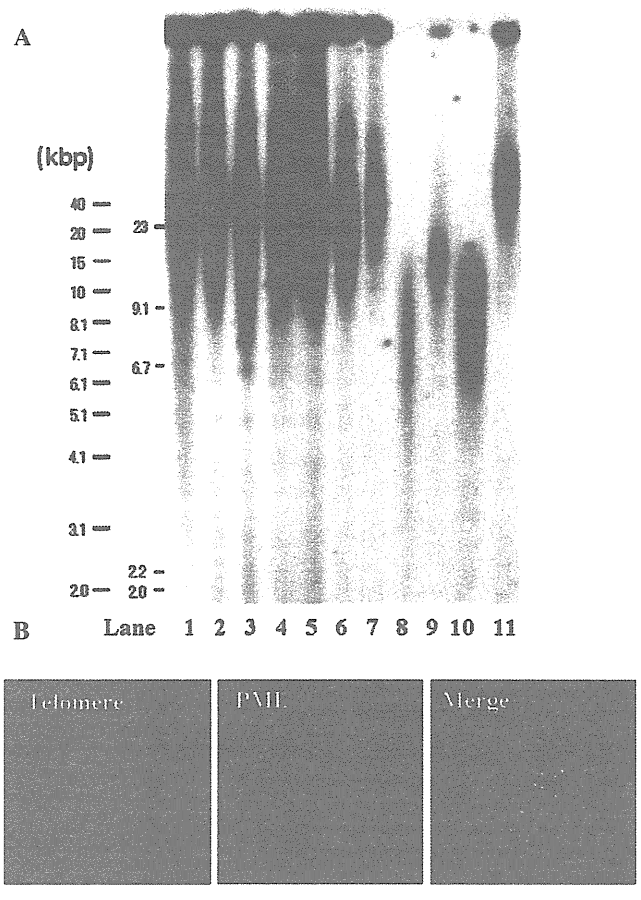

Figure 2. (A), Telomere lengths in hMSCs. Terminal restriction fragment lengths were measured by Southern blot analysis using pulse-field gel electrophoresis. Lane 1, hMSC#3 (+FGF) 15.2 PDL; lane 2, hMSC#3 (+FGF) 318.9 PDL; lane 3, hMSC#3 (+FGF) 501.6 PDL; lane 4, hMSC#4 (+FGF) 55 PDL; lane 5, hMSC#4 (+FGF) 105.3 PDL; lane 6, hMSC#4 (+FGF) 554.6 PDL; lane 7, TERT-transfected hMSC#4 484.6 PDL; lane 8, hMSC#3 (-FGF) 24.6 PDL; lane 9, hMSC#3 (-FGF) 46.4 PDL; lane 10, hMSC#4 (-FGF) 26.2 PDL; lane 11, TERT-transfected hMSC#3 426.2 PDL. (B), Confocal imaging showing the nuclear expression patterns in the telomere (Cy3 labeled) and promyelocytic leukemia (PML) body-related antigen mAb (FITC labeled). hMSC#3 (+FGF) 318.9 PDL demonstrated strong telomeric signals and large PML bodies. Both signals merged in the nuclei.

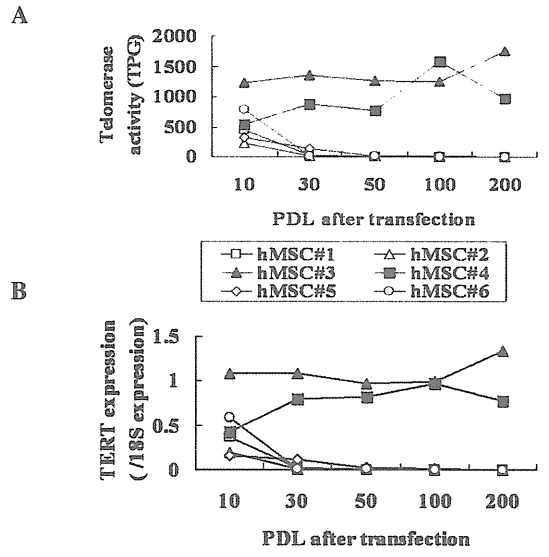

Figure 3. Telomerase activity and TERT expression in TERT transfected hMSCs. (A), In the 6 TERT transfected clones, telomerase activity was diminished in four clones (0.2-1.31 TPG in hMSC lines #1, #2, #5, and #6) and retained in two (1761.3 and 965.3 TPG in hMSC lines #3, and #4, respectively). (B), TERT expression were also retained in these two clones but diminished in the remaining 4 clones.

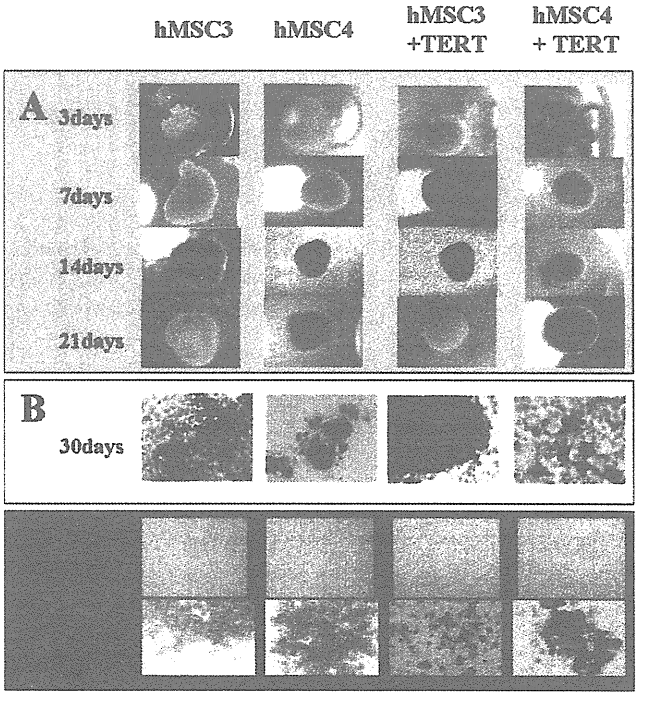

Figure 4. Induction of hMSC differentiation. (A), Macroscopic view of chondrogenesis. Pellet culture of FGF(+) MSC-derived pellets at 3, 7, 14, and 21 days. (B), Microscopic views of adipogenesis. Oil Red-O staining of FGF(+) MSC-derived pellets at 3, 7, 14, and 21 days. (C), Microscopic views of osteogenesis of hMSCs.

stimulated in lineage-specific induction medium for 2-4 weeks (Fig. 4). In adipocyte-specific culture medium, all of the cell lines accumulated lipid-rich vacuoles in their cytoplasm within 2 weeks, which were made evident by Oil Red-O staining. After 3 weeks in chondrocyte differentiation media, hMSCs and TERT-transfected hMSCs had metachromasia by TB and expression of type II collagen. After culturing cells as a micromass pellet for 21 days, the size of the TERT-transfected hMSCs was slightly smaller those of the parent hMSCs, but both had differentiated into cartilage (Fig. 4A) and, both hMSCs and TERT-transfected hMSCs showed greater adipogenetic ability (Fig. 4B). After 2 weeks in osteoblast induction medium, hMSCs and TERT-transfected hMSCs showed a marked increase in alkaline phosphatase expression (Fig. 4C), an osteoblast marker TERT-transfected immortalized mesenchymal stem cell lines retained the ability to differentiate into three lineages, although among cell lines there were significant variations in response to lineage-specific induction.

TERT enhanced the colony-forming ability of hMSCs. The colony formation assay revealed that colony numbers formed in soft agar were highly correlated with *TERT* expression levels in hMSCs. The colony numbers in TERT-transfected hMSC clones (hMSC#3 and #4) were significantly higher than

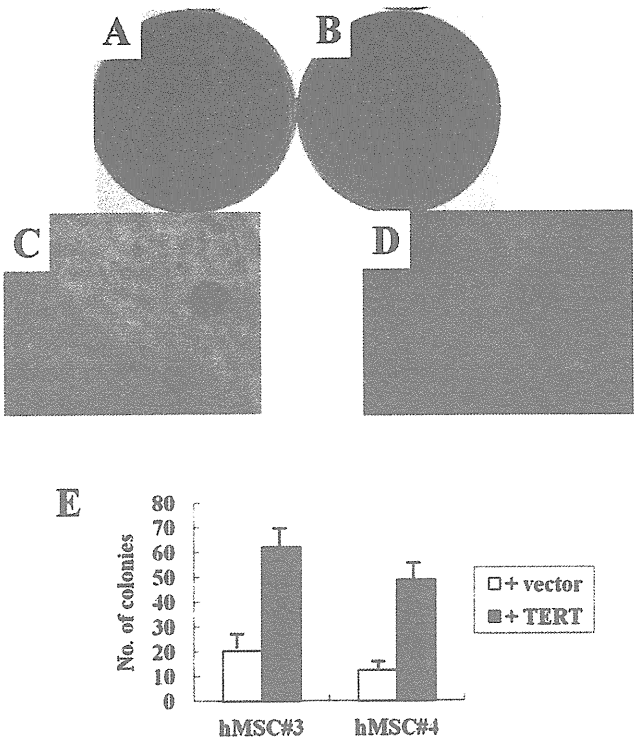

Figure 5. Soft agar assay of hMSCs colony numbers at day 21 in colony formation assay with soft agar for a vector-transfected clone (hMSC#3+vector) (A) and TERT-transfected clone (hMSC#3+TERT) (B). Both colony types were stained with crystal violet. Colonies formed from TERT-transfected clones (D) were significantly larger than those of the vector transfected clone (C). (E), Bar graph showed the difference of colony formation between the vector and TERT-transfected clones in hMSC#3 and #4.

Table I. Xenograft and tumor growth in NOD/SCID injected with hMSCs.

hMSCs	No. of cells injected	Tumor formation (tumor volume, mm^3)
TERT-hMSCs		
#1	100	0/4
	100000	0/4
#2	100	0/4
	100000	1/4 (648)
#3	100	2/4 (765, 546)
	100000	4/4 (8740, 4080, 3504, 3360)
#4	100	3/4 (1728, 1200, 855)
	100000	4/4 (12000, 4560, 3420)
#5	100	0/4
	100000	3/4 (1872, 966, 742)
#6	100	0/4
	100000	0/4
Vector-hMSCs		
#1-6	100	0/12
#1	100000	0/4
#2	100000	2/4 (1560, 540)
#3	100000	1/4 (874)
#4	100000	0/4
#5	100000	0/4
#6	100000	0/4

those of hMSCs without detectable *TERT* expression ($P<0.001$). In addition, the cellular growth rates of TERT-transfected hMSC (hMSC#3 and #4) clones are higher than those of vector-transfected clones (Fig. 5).

In vivo tumorigenic assays. TERT-transfected hMSC cells (10^2 or 10^5) were subcutaneously injected into NOD-*scid* mice and tumor development was evaluated. As shown in Table I and Fig. 6, all mice injected with 10^5 cells of *TERT*-expressing hMSC clones (*TERT*-hMSC#3 and *TERT*-hMSC#4) developed tumors and 5 of 8 mice injected with 10^2 cells of these *TERT*-expressing hMSC clones developed tumors. In contrast, four other TERT-transfected hMSC clones (*TERT*-hMSC#1, #2, #5, and #6) and all the vector-transfected hMSCs, did not produce tumors after injections of 10^2 cells, although an injection of two vector-transfected hMSCs clones (*vector*-hMSC#2 and *vector*-hMSC#3) and two TERT-transfected hMSC clones (*TERT*-hMSC#2 and *TERT*-hMSC#5) did induce tumorigenesis in mice after 10^5 injection (Table I).

Macroscopically, tumors derived from TERT-expressing hMSCs (*TERT*-hMSC#3 and *TERT*-hMSC#4) were large and hard (Fig. 6B), while tumors arising from cells without TERT expression were small and relatively soft (Fig. 6F). Histological examination revealed that the former were teratocarcinoma-like tumors (Fig. 6C and D), while the latter were teratomas with several differentiated tissues, including fat and bone (Fig. 6G and H). Immunohistological examination revealed that the former showed TERT expression (Fig. 6E), while the latter did not (Fig. 6I).

Discussion

hMSCs maintain the homeostasis of bone and cartilage and are found in adult human BM. Those obtained from human in late adulthood still exhibit osteogenic potency (15). Thus, it is thought that hMSCs maintain lifetime self-renewal and differentiation capacity *in vivo*. However, several previous studies showed that the self-renewal potency of hMSCs is decreased by long-term culture *in vitro* (16-18) and that FGF-2 expands multipotent hMSCs with high proliferation potential (7). It is also possible that cellular senescence in hMSCs, which might be induced by TGF-β1 and increased levels of CDK inhibitors ($p16^{INK4a}$, $p21^{Cip1}$, and p53), is reversed by FGF-2 (19,20). In the present study, six FGF(+) hMSC clones were cultureable for more than one year. The mechanism by which they were immortalized is still unknown, but these cell lines retain muti-potential differentiation activity. Thus, these human BM-derived MSCs can be cultured long-term *in vitro*, without losing their peculiar morphological, phenotypical, and functional characteristics and might become a universal source of cells for regenerative therapies. To elucidate the mechanism of immortalization, we analyzed telomere and telomerase in these immortalized hMSCs. Long telomere lengths (approximately 40 kb) were maintained without detectable telomerase activity.

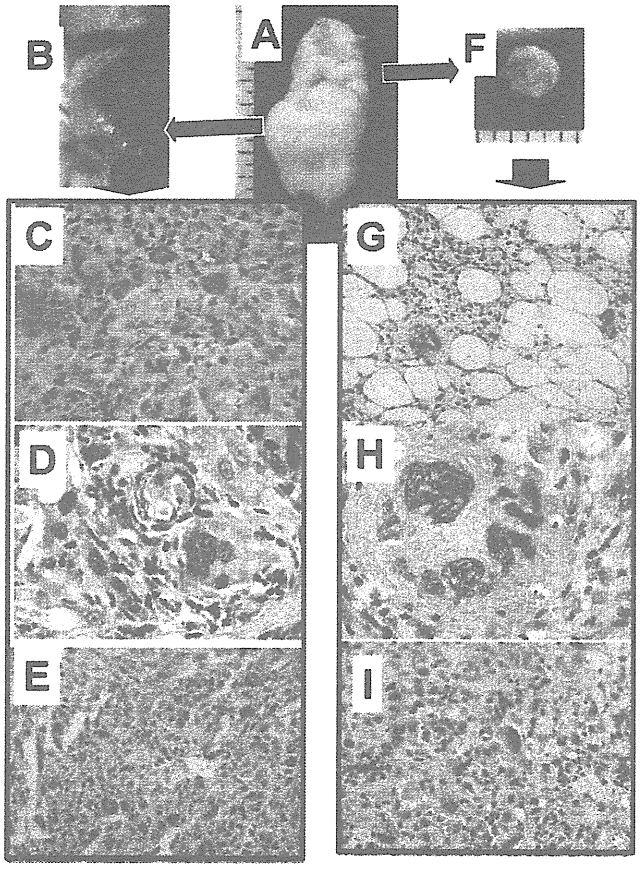

Figure 6. Tumor formation in NOD/SCID mice. (A), Subcutaneous transplantation of 10^2 TERT-transfected hMSC#3 (left side) and 10^5 vector-transfected hMSC#3 (right side) in NOD mice. (B), Subcutaneous transplantation of TERT-transfected hMSC#3 (10^2 cells) developed large tumor formation. (C), Histological findings of this tumor showed teratocarcinoma without differentiated cells. (D), In this tumor, vascular invasion and polynuclear cells were determined. (E), Immunohistological examination of TERT revealed that most tumor cells were positive. (F), In contrast, subcutaneous transplantation of vector-transfected hMSC#3 (10^5 cells) developed a soft tumor. (G and H), This tumor showed teratoma with differentiated cells such as adipose and cartilage. (I), This tumor did not contain TERT expressing cells.

Thus, telomeres in these cells are maintained by ALT, which is characterized phenotypically by long and heterogeneous telomeres. ALT-activated tumors, relatively low in human malignancies, are sometimes of mesenchymal origin, and there is evidence to suggest an MSC origin for ALT immortalization in cell lines (21). Therefore, ALT activation of these hMSCs might be characteristic of the mesenchymal origin cells.

Telomerase activity and TERT expression were repressed in our hMSCs clones, even after the cells acquired immortalization. Their repression occurred in ALT-activated hMSCs, although there were several instances of hMSCs with telomerase activation to maintain telomere length for acquiring immortalization (20,22). Thus, two mechanisms based on the presence of either telomerase or ALT expression influence hMSC immortalization. Several reports of hMSC immortalization via TERT transduction, and the present data describing immortalization in FGF-2-expanded hMSCs via an ALT mechanism, support this discrimination. However, the mechanism of these activation on hMSCs *in vivo* remains unknown and the effects of both factors at the same time on hMSCs are unclear.

In the present study, human BM-derived MSCs could be cultured long-term in medium with FGF-2 without losing their peculiar morphological, phenotypical, and functional characteristics. TERT-transfected hMSCs retain the potential of chondrogenic, osteogenic, and adipogenic differentiation but display an increased capacity of colony formation in soft agar and increased tumorigenicity in immunodeficient mice. The transduction of TERT obviously induces the malignant phenotypes of hMSCs, which can also be cultured long-term *in vitro*, without loss of their morphological, phenotypical, and functional characteristics. In these TERT-transfected clones, hMSCs that express TERT exhibit malignant phenotypes, while those that lose TERT expression do not. Therefore, TERT transduction might play a significant role in the malignant transformation of hMSCs. Although telomerase activity was upregulated in TERT-transfected clones, telomere lengths were as long as those in ALT-activated clones before TERT transfection, indicating that transduced TERT might play a role in malignant transformation other than telomere maintenance. Recent reports suggest that TERT is active in a wide variety of functions, and is a component of RNA-dependent RNA polymerase (23). Therefore, activation of TERT might correlate with malignant transformation of hMSCs. TERT-transduced hMSCs also have extended replicative capacity while maintaining their differential capacity (22,24). Therefore, since our hMSCs were immortalized by ALT after FGF-2 treatment before TERT transfection, other factors might be necessary for malignant transformation of normal hMSCs.

In conclusion, human BM-derived MSCs can be cultured long-term *in vitro* by ALT telomere maintenance without losing their morphological, phenotypical, and functional characteristics. Moreover, these cells are malignantly transformed by TERT transduction, suggesting that activation of TERT is correlated with cancer formation of hMSCs. These cells might be a model for cancer stem cells if they derive from normal tissue stem cells. Further studies are necessary to fully understand the mechanism of malignant transformation by TERT transduction and any correlation with cancer stem cells. Our results support the concept that the biological properties of hMSCs after *in vitro* expansion remain suitable for use in cell therapy approaches; however, considering the interest in the utilization of hMSCs in several fields of medicine and the potential risk of developing malignant transformation during the expansion period, we strongly recommended the establishment of a suitable test for phenotypic, functional, and genetic characteristics of hMSCs after *in vitro* expansion to further guarantee the safety of the patient.

Acknowledgements

We thank Professor M. Ochi and other surgeons and orthopedic surgeons in Graduate School of Biomedical Sciences, Hiroshima University for providing clinical support for this study. This research was partially supported by a Grant-in-Aid for Scientific Research (B) (Nos. 19390449. 21390474 and 22700917) and (Hoga) (19659324 and 20659198) from the Ministry of Education, Culture, Sports, Science, and Technology and those from the Ministry of Health, Labor, and Welfare of the Government of Japan.

References

1. Okamoto T, Aoyama T, Nakayama T, Nakamata T, Hosaka T, Nishijo K, Nakamura T, Kiyono T and Toguchida J: Clonal heterogeneity in differentiation potential of immortalized human mesenchymal stem cells. Biochem Biophys Res Commun 295: 354-361, 2002.
2. Takeda Y, Mori T, Imabayashi H, Kiyono T, Gojo S, Miyoshi S, Hida N, Ita M, Segawa K, Ogawa S, Sakamoto M, Nakamura S and Umezawa A: Can the life span of human marrow stromal cells be prolonged by bmi-1, E6, E7, and/or telomerase without affecting cardiomyogenic differentiation? J Gene Med 6: 833-845, 2004.
3. Mori T, Kiyono T, Imabayashi H, Takeda Y, Tsuchiya K, Miyoshi S, Makino H, Matsumoto K, Saito H, Ogawa S, Sakamoto M, Hata J and Umezawa A: Combination of hTERT and bmi-1, E6, or E7 induces prolongation of the life span of bone marrow stromal cells from an elderly donor without affecting their neurogenic potential. Mol Cell Biol 25: 5183-5195, 2005.
4. Saito M, Handa K, Kiyono T, Hattori S, Yokoi T, Tsubakimoto T, Harada H, Noguchi T, Toyoda M, Sato S and Teranaka T: Immortalization of cementoblast progenitor cells with Bmi-1 and TERT. J Bone Miner Res 20: 50-57, 2005.
5. Terai M, Uyama T, Sugiki T, Li XK, Umezawa A and Kiyono T: Immortalization of human fetal cells: the life span of umbilical cord blood-derived cells can be prolonged without manipulating p16INK4a/RB braking pathway. Mol Biol Cell 16: 1491-1499, 2005.
6. Tsutsumi S, Shimazu A, Miyazaki K, Pan H, Koike C, Yoshida E, Takagishi K and Kato Y: Retention of multilineage differentiation potential of mesenchymal cells during proliferation in response to FGF. Biochem Biophys Res Commun 288: 413-419, 2001.
7. Yanada S, Ochi M, Kojima K, Sharman P, Yasunaga Y and Hiyama E: Possibility of selection of chondrogenic progenitor cells by telomere length in FGF-2-expanded mesenchymal stromal cells. Cell Prolif 39: 575-584, 2006.
8. Hiyama E, Yokoyama T, Hiyama K, Michio Y, Santo T, Kodama T, Ichikawa T and Matsuura Y: Alteration of telomeric repeat length in adult and childhood solid neoplasias. Int J Oncol 6: 13-16, 1995.
9. Hiyama K, Ishioka S, Shirotani Y, Inai K, Hiyama E, Murakami I, Isobe T, Inamizu T and Yamakido M: Alterations in telomeric repeat length in lung cancer are associated with loss of heterozygosity in p53 and Rb. Oncogene 10: 937-944, 1995.
10. Kim NW, Piatyszek MA, Prowse KR, Harley CB, West MD, Ho PLC, Coviello GM, Wright WE, Weinrich SL and Shay JW: Specific association of human telomerase activity with immortal cells and cancer. Science 266: 2011-2015, 1994.
11. Piatyszek MA, Kim NW, Weinrich SL, Hiyama K, Hiyama E, Wright WE and Shay JW: Detection of telomerase activity in human cells and tumors by a telomeric repeat amplification protocol (TRAP). Methods Cell Sci 17: 1-15, 1995.
12. Chromczynski P and Sacchi N: Single-step method of RNA isolation by acid guanidinium thiocyanate-phenol-chloroform extraction. Anal Biochem 162: 156-159, 1987.
13. Hiyama E, Hiyama K, Shay JW and Yokoyama T: Immunohistochemical detection of telomerase (hTERT) protein in human cancer tissues and a subset of cells in normal tissues. Neoplasia 3: 17-26, 2001.
14. Pittenger MF, Mackay AM, Beck SC, Jaiswal RK, Douglas R, Mosca JD, Moorman MA, Simonetti DW, Craig S and Marshak DR: Multilineage potential of adult human mesenchymal stem cells. Science 284: 143-147, 1999.
15. Radio NM, Doctor JS and Witt-Enderby PA: Melatonin enhances alkaline phosphatase activity in differentiating human adult mesenchymal stem cells grown in osteogenic medium via MT2 melatonin receptors and the MEK/ERK (1/2) signaling cascade. J Pineal Res 40: 332-342, 2006.
16. Jaiswal N, Haynesworth SE, Caplan AI and Bruder SP: Osteogenic differentiation of purified, culture-expanded human mesenchymal stem cells *in vitro*. J Cell Biochem 64: 295-312, 1997.
17. Deans RJ and Moseley AB: Mesenchymal stem cells: biology and potential clinical uses. Exp Hematol 28: 875-884, 2000.
18. Jiang Y, Jahagirdar BN, Reinhardt RL, Schwartz RE, Keene CD, Ortiz-Gonzalez XR, Reyes M, Lenvik T, Lund T, Blackstad M, Du J, Aldrich S, Lisberg A, Low WC, Largaespada DA and Verfaillie CM: Pluripotency of mesenchymal stem cells derived from adult marrow. Nature 418: 41-49, 2002.
19. Bianchi G, Banfi A, Mastrogiacomo M, Notaro R, Luzzatto L, Cancedda R and Quarto R: Ex vivo enrichment of mesenchymal cell progenitors by fibroblast growth factor 2. Exp Cell Res 287: 98-105, 2003.
20. Zhang X, Soda Y, Takahashi K, Bai Y, Mitsuru A, Igura K, Satoh H, Yamaguchi S, Tani K, Tojo A and Takahashi TA: Successful immortalization of mesenchymal progenitor cells derived from human placenta and the differentiation abilities of immortalized cells. Biochem Biophys Res Commun 351: 853-859, 2006.
21. Lafferty-Whyte K, Cairney CJ, Will MB, Serakinci N, Daidone MG, Zaffaroni N, Bilsland A and Keith WN: A gene expression signature classifying telomerase and ALT immortalization reveals an hTERT regulatory network and suggests a mesenchymal stem cell origin for ALT. Oncogene 28: 3765-3774, 2009.
22. Simonsen JL, Rosada C, Serakinci N, Justesen J, Stenderup K, Rattan SI, Jensen TG and Kassem M: Telomerase expression extends the proliferative life-span and maintains the osteogenic potential of human bone marrow stromal cells. Nat Biotechnol 20: 592-596, 2002.
23. Maida Y, Yasukawa M, Furuuchi M, Lassmann T, Possemato R, Okamoto N, Kasim V, Hayashizaki Y, Hahn WC and Masutomi K: An RNA-dependent RNA polymerase formed by TERT and the RMRP RNA. Nature 461: 230-235, 2009.
24. Shi S, Gronthos S, Chen S, Reddi A, Counter CM, Robey PG and Wang CY: Bone formation by human postnatal bone marrow stromal stem cells is enhanced by telomerase expression. Nat Biotechnol 20: 587-591, 2002.

OBSERVATIONS

Pancreatic β-Cell Function in Women With Gestational Diabetes Mellitus Defined by New Consensus Criteria

A potential etiology for gestational diabetes mellitus (GDM) is a limitation in β-cell reserves that manifests as hyperglycemia when insulin secretion does not increase to match the escalated insulin needs during pregnancy (1). Recently, the international association of diabetes and pregnancy study groups (IAPDSG) proposed new criteria for diagnosing and classifying diabetes in pregnancy based on the association of maternal hyperglycemia with perinatal outcomes (2). To date, β-cell function in GDM defined by the new consensus criteria has not been reported. β-cell function has been assessed by a disposition index defined as the product of insulin sensitivity and insulin secretion determined by intravenous glucose tolerance test (IVGTT) (3). The recent demonstration of a hyperbolic relation between indexes of insulin secretion and insulin sensitivity from the oral glucose tolerance test (OGTT) has led to the introduction of novel OGTT-derived measures of β-cell function analogous to the disposition index (4). Therefore, we assessed β-cell function in Japanese women with GDM using the OGTT-derived measures (i.e., oral disposition index [DIo]). Of the 2,267 sequential women who underwent universal screening for GDM from January 2004 to February 2010, 409 with positive 1-h 50-g glucose challenge test results had a standard 2-h 75-g OGTT. Venous blood samples for the measurement of plasma glucose level (mg/dl) and insulin concentration (μU/ml) were drawn in the fasting state, at 30 min, 1 h, and 2 h after ingestion of the glucose drink. The ratio of the insulin area under the curve to the glucose area under the curve multiplied by the composite index of insulin sensitivity during the OGTT was used as the DIo in this study. With the IAPDSG criteria, 126 women were diagnosed as GDM: 58 with single abnormal value, 50 with two abnormal values, and 18 with three abnormal values. Of the 126 GDM women, 101 (80%) were identified by the fasting glucose plus 1-h plasma glucose levels. The natural log-transformed DIo in GDM was significantly lower than that in non-GDM (mean ± SD, 1.69 ± 0.57 vs. 2.59 ± 0.96, $P < 0.0001$). Similar to women with two or three abnormal OGTT values (1.62 ± 0.35 and 1.06 ± 0.38, respectively), those with a single abnormal value exhibited significantly lower levels of DIo (1.96 ± 0.59) compared with those with non-GDM ($P < 0.001$). After adjustment for prepregnancy BMI, family history of diabetes, and the glucose intolerance status (i.e., GDM) using multiple linear regression model, GDM was still a negative correlate of the DIo ($P < 0.0001$).

Consistent with the IADPSG analysis, fasting plus 1-h plasma glucose levels identified the majority of GDM women. Using the DIo, β-cell dysfunction was demonstrated in women with GDM defined by the IAPDSG criteria. Previous studies indicate that β-cell function determined by the disposition index from OGTT as well as IVGTT is predictive of the development of diabetes (5). Our findings suggest that the women with GDM identified using the new consensus criteria are at high risk of development of subsequent diabetes, as well as adverse perinatal outcomes.

Acknowledgments— No potential conflicts of interest relevant to this article were reported.

The authors are grateful to Drs. Keisuke Kouyama and Takayuki Abe of Center for Clinical Research, Keio University School of Medicine, for their valuable statistical assistance.

KEI MIYAKOSHI, MD[1]
YOSHIFUMI SAISHO, MD[2]
MAMORU TANAKA, MD[1]
AKIRA SHIMADA, MD[3]
HIROSHI ITOH, MD[2]
YASUNORI YOSHIMURA, MD[1]

From the [1]Department of Obstetrics and Gynecology, School of Medicine, Keio University, Tokyo, Japan; the [2]Department of Internal Medicine, School of Medicine, Keio University, Tokyo, Japan; and the [3]Division of Internal Medicine, Tokyo Saiseikai Central Hospital, Tokyo, Japan.

Corresponding author: Kei Miyakoshi, kei@sc.itc.keio.ac.jp.

DOI: 10.2337/dc10-1725

References

1. Buchanan TA, Xiang AH. Gestational diabetes mellitus. J Clin Invest 2005;115:485–491
2. International Association of Diabetes and Pregnancy Study Groups Consensus Panel, Metzger BE, Gabbe SG, Persson B, Buchanan TA, Catalano PA, Damm P, Dyer AR, Leiva A, Hod M, Kitzmiler JL, Lowe LP, McIntyre HD, Oats JJ, Omori Y, Schmidt MI. International association of diabetes and pregnancy study groups recommendations on the diagnosis and classification of hyperglycemia in pregnancy. Diabetes Care 2010;33:676–682
3. Bergman RN, Ader M, Huecking K, Van Citters G. Accurate assessment of beta-cell function: the hyperbolic correction. Diabetes 2002;51 (Suppl 1):S212–S220
4. Retnakaran R, Shen S, Hanley AJ, Vuksan V, Hamilton JK, Zinman B. Hyperbolic relationship between insulin secretion and sensitivity on oral glucose tolerance test. Obesity 2008;16:1901–1907
5. Utzschneider KM, Prigeon RL, Faulenbach MV, Tong J, Carr DB, Boyko EJ, Leonetti DL, McNeely MJ, Fujimoto WY, Kahn SE. Oral disposition index predicts the development of future diabetes above and beyond fasting and 2-h glucose levels. Diabetes Care 2009;32:335–341

Paracrine IL-33 Stimulation Enhances Lipopolysaccharide-Mediated Macrophage Activation

Tatsukuni Ohno[1,2], Keisuke Oboki[1], Hideaki Morita[1], Naoki Kajiwara[1,3], Ken Arae[1], Shizuko Tanaka[4], Masako Ikeda[4], Motoyasu Iikura[5], Taishin Akiyama[6], Jun-ichiro Inoue[6], Kenji Matsumoto[1], Katsuko Sudo[9], Miyuki Azuma[2], Ko Okumura[3], Thomas Kamradt[10], Hirohisa Saito[1,3], Susumu Nakae[1,3,7,8]*

1 Department of Allergy and Immunology, National Research Institute for Child Health and Development, Tokyo, Japan, 2 Department of Molecular Immunology, Graduate School of Medical and Dental Science, Tokyo Medical and Dental University, Tokyo, Japan, 3 Atopy Research Center, Juntendo University, Tokyo, Japan, 4 Technical and Research Department, Ina Laboratory, Medical and Biological Laboratories Co., Ltd., Nagano, Japan, 5 Department of Respiratory Medicine, International Medical Center of Japan, Tokyo, Japan, 6 Division of Cellular and Molecular Biology, The Institute of Medical Science, The University of Tokyo, Tokyo, Japan, 7 Frontier Research Initiative, The Institute of Medical Science, The University of Tokyo, Tokyo, Japan, 8 Laboratory of Systems Biology, Center for Experimental Medicine and Systems Biology, The Institute of Medical Science, The University of Tokyo, Tokyo, Japan, 9 Animal Research Center, Tokyo Medical University, Tokyo, Japan, 10 Institut für Immunologie, Universitätsklinikum Jena, Jena, Germany

Abstract

Background: IL-33, a member of the IL-1 family of cytokines, provokes Th2-type inflammation accompanied by accumulation of eosinophils through IL-33R, which consists of ST2 and IL-1RAcP. We previously demonstrated that macrophages produce IL-33 in response to LPS. Some immune responses were shown to differ between ST2-deficient mice and soluble ST2-Fc fusion protein-treated mice. Even in anti-ST2 antibody (Ab)-treated mice, the phenotypes differed between distinct Ab clones, because the characterization of such Abs (i.e., depletion, agonistic or blocking Abs) was unclear in some cases.

Methodology/Principal Findings: To elucidate the precise role of IL-33, we newly generated neutralizing monoclonal Abs for IL-33. Exogenous IL-33 potentiated LPS-mediated cytokine production by macrophages. That LPS-mediated cytokine production by macrophages was suppressed by inhibition of endogenous IL-33 by the anti-IL-33 neutralizing mAbs.

Conclusions/Significance: Our findings suggest that LPS-mediated macrophage activation is accelerated by macrophage-derived paracrine IL-33 stimulation.

Citation: Ohno T, Oboki K, Morita H, Kajiwara N, Arae K, et al. (2011) Paracrine IL-33 Stimulation Enhances Lipopolysaccharide-Mediated Macrophage Activation. PLoS ONE 6(4): e18404. doi:10.1371/journal.pone.0018404

Editor: Lena Alexopoulou, Centre d'Immunologie de Marseille-Luminy, CNRS-Inserm, France

Received September 29, 2010; **Accepted** March 7, 2011; **Published** April 11, 2011

Funding: This work was supported by the Japan Chemical Industry Association, Grants-in-Aid for Young Scientists (B) (T.O., K. Oboki. and S.N.), the Program for Improvement of Research Environment for Young Researchers, The Special Coordination Funds for Promoting Science and Technology (S.N.) from the Ministry of Education, Culture, Sports, Science and Technology, Japan and a grant from the National Institute of Biomedical Innovation (H.S.). S.T. and M.I., who are the researchers in Medical & Biological Laboratories Co., Ltd., generated the anti-IL-33 mAb in the submitted manuscript. The other funders had no role in study design, data collection and analysis, decision to publish, or preparation of the manuscript.

Competing Interests: The authors have declared that no competing interests exist.

* E-mail: snakae@ims.u-tokyo.ac.jp

Introduction

IL-33 (also called IL-1F11, DVS27 and NF-HEV), which is a member of the IL-1 family of cytokines that includes IL-1 and IL-18, was identified as a ligand for ST2 (also called T1, DER-4, Fit-1 and IL-1R4) [1,2,3,4]. IL-33 is considered to be a cytokine that potently induces production of such Th2-cytokines as IL-5 and IL-13 by ST2-expressing immune cells such as Th2 cells [1,5,6], mast cells [7,8,9,10,11], eosinophils [6,12,13], basophils [12,13,14] and macrophages [15,16], and by stem-cell-like cells such as $CD34^+$ hematopoietic stem cells [17], natural helper cells [18] and nuocytes [19]. IL-33 is thereby thought to contribute to the development of Th2-cytokine-associated immune responses, including host defense against nematode infection and allergic diseases [2,3,4].

Indeed, administration of IL-33 to mice resulted in increased serum levels of Th2-cytokines such as IL-4, IL-5 and IL-13, as well as IgG1 and IgE, and development of inflammation accompanied by accumulation of eosinophils in the lung and gut [1]. Moreover, polymorphism of the ST2 and/or IL-33 genes was found in patients with asthma [20,21,22], atopic dermatitis [23], rhinitis [24] and rhinosinusitis [25]. The mRNA and/or protein levels of ST2, soluble ST2, which acts as a decoy receptor for IL-33, and IL-33 are increased in specimens from patients with allergic diseases such as asthma [26,27,28,29,30,31], conjunctivitis [31], rhinitis [24] and atopic dermatitis [32]. Therefore, these observations strongly suggest the importance of IL-33 and ST2 for the development of Th2-cytokine-associated allergic disorders.

However, based on the results of a study using mice treated with anti-ST2 Ab or soluble ST2-Fc fusion proteins and/or deficient in ST2, the roles of IL-33 and ST2 in the pathogenesis of certain immune diseases, including allergic airway inflammation, remain controversial [4]. Studies using ST2-deficient mice found that ovalbumin (OVA)-induced airway inflammation developed nor-

mally in ST2-deficient mice sensitized twice with OVA emulsified with alum [33,34,35], whereas it was attenuated in the case of a single sensitization [35]. On the other hand, mice treated with anti-ST2 mAb clone "3E10," which induced Th2 cell activation as an agonistic Ab, at least *in vitro* [36], without depleting ST2-expressing cells *in vivo* [37], and mice treated with soluble ST2 showed reduced development of OVA-induced airway inflammation, even though they were sensitized twice with OVA with alum [38,39]. Unlike in ST2-deficient mice [33,34,35], the development of OVA-induced airway inflammation was aggravated in mice injected with ST2-deficient OVA-specific TCR (DO11.10)-expressing Th2 cells in comparison with those injected with wild-type DO11.10 Th2 cells after OVA challenge [34]. That finding suggests that ST2 plays a negative role in Th2 cells, at least in that setting. On the other hand, it was shown that administration of anti-ST2 mAb "3E10" and soluble ST2-Fc fusion proteins to mice injected with DO11.10 Th2 cells resulted in attenuation of OVA-induced airway inflammation [38,40]. These seemingly contradictory observations could be explained on the basis of different roles for IL-33 and ST2 in distinct ST2-expressing cells. In support of that concept, IL-33 is able to enhance IFN-γ production by NK cells and iNKT cells [26], which are also involved in the pathogenesis of allergic airway inflammation [41,42]. Therefore, the precise roles of IL-33 and ST2 in different types of cells need to be elucidated.

We and others have demonstrated that IL-33 is able to enhance cytokine secretion by mast cells [7,9] and macrophages [43]. We also reported that both mast cells and macrophages can produce IL-33 after stimulation with IgE and LPS, respectively [44]. These observations suggest that IL-33 may be involved in the activation of these cells by autocrine/paracrine IL-33 release after such stimulation. In the present study, we used newly generated anti-IL-33 mAbs and demonstrated that activation of macrophages, but not mast cells, was modulated by paracrine IL-33 stimulation.

Materials and Methods

Mice

BALB/cA (BALB) mice, C57BL/6J (B6J) mice and C57BL/6N (B6N) mice were purchased from CLEA Japan and Sankyo Lab, respectively. B6J-TLR4$^{-/-}$ mice [45] and BALB-ST2$^{-/-}$ mice [46] were kindly provided by Drs. Tsuneyasu Kaisho (RIKEN, Japan) and Andrew N.J. McKenzie (MRC, Cambridge, UK), respectively. B6J-TRAF6$^{-/-}$ mice [47] and B6N-IL-33$^{-/-}$ mice [48] were generated as described elsewhere. All mice were housed under specific-pathogen-free conditions in our institutes (National Research Institute for Child Health and Development or The Institute of Medical Science, The University of Tokyo), and the animal protocols were approved by the Institutional Review Board of the National Research Institute for Child Health and Development (#06-10) and The Institute of Medical Science, The University of Tokyo (#A09-10).

Anti-mouse ST2 Abs

Anti-mouse ST2 mAb (clone 3E10) had been generated as described elsewhere [40]. FITC-conjugated and non-conjugated anti-mouse ST2 mAbs (clones DJ8 [49,50], 245707 and 245714) were obtained from MD Bioscience and R&D Systems, respectively.

Anti-IL-33 Abs

Anti-human/mouse IL-33 mAb (Nessy-1, Alexis), anti-mouse IL-33 mAb (518017, R&D Systems) and anti-mouse IL-33 polyAb (AF3626, R&D Systems) were used.

Generation of anti-mouse IL-33 mAbs

Anti-mouse IL-33 mAbs were generated and provided by Medical & Biological Laboratories Co., Ltd. (Nagano, Japan). cDNA encoding the mouse IL-33 corresponding to amino acids 109–266 was expressed in *E. coli* as an N-terminal tagged fusion protein. After purification of the fusion protein, the tagged sequence was cleaved enzymatically and removed by affinity purification. Five-week-old female C3H mice (Japan SLC, Hamamatsu) were immunized with the purified protein emulsified with Freund's complete adjuvant (Sigma-Aldrich) by injection into the footpads 5 times at 1-week intervals]. Three days after the final immunization, cells from the lymph nodes of the immunized mice were fused with P3-U1 mouse myeloma cells in the presence of 50% (w/v) polyethylene glycol (PEG4000) (Wako). Hybridomas were screened by ELISA and immunoblotting to identify those generating mAbs. Positive clones were subcloned two times by limiting dilution and rescreened by ELISA and immunoblotting. The mAbs were purified from the culture supernatant using Protein A-Sepharose (GE Healthcare). The eluted antibodies were analyzed by SDS-PAGE.

Bone marrow cell-derived and fetal liver cell-derived cultured mast cells

Mouse femoral bone marrow cell-derived cultured mast cells (BMCMCs) were generated as described elsewhere [7]. For generation of fetal liver cell-derived cultured mast cells (FLCMCs), livers were harvested from newborn TRAF6$^{+/+}$ and TRAF6$^{-/-}$ mice, and liver single-cell suspensions were prepared by grinding the tissues through a 70-μm nylon cell strainer (BD Falcon) with the plunger of a 5-ml disposable syringe. Bone marrow cells and fetal liver cells were cultured in the presence of 10 ng/ml rmIL-3 (PeproTech) for 6–8 weeks, at which time flow cytometry showed the cells to be a >98% c-kit$^+$ FcεRIα$^+$ population. Before using the cells, rmIL-3 was removed by washing. MCs (2×10^5 cells/well in 96-well flat-bottom plates) were cultured with 1 μg/ml IgE (SPE-7, Sigma), 30 or 100 ng/ml rmIL-33 (R&D Systems) and a combination of 1 μg/ml SPE-7 plus 100 ng/ml rmIL-33 in the presence and absence of 40 or 80 μg/ml anti-mouse ST2 mAb, anti-IL-33 Ab or isotype-matched control IgG for 24 h.

Thioglycolate (TGC)-induced macrophages

For collection of thioglycolate (TGC)-induced mouse peritoneal macrophages (TGC-macrophages), mice were injected intraperitoneally with 5 ml of 2% TGC (Nissui). Three days later, peritoneal exudate cells (PECs) were collected. TGC-macrophages (2×10^5 cells/well in 96-well flat-bottom plates) were incubated with 0–100 ng/ml LPS (*Salmonella enterica* serotype typhimurium; SIGMA) in the presence and absence of 40 μg/ml anti-ST2 mAb, anti-IL-33 mAb or isotype-matched control IgG for 24 or 48 h.

Flow cytometry

BMCMCs were incubated with anti-CD16/CD32 mAb (93, eBioscience; or 2.4G2, BD Biosciences) for 15 min on ice. The cells were then incubated with PE-conjugated anti-mouse FcεRIα (MAR-1, eBioscience), APC-conjugated anti-mouse c-Kit (2B8, eBioscience) and FITC-conjugated or non-conjugated anti-mouse ST2 mAb (DJ8, 3E10, 245707 or 245714) for 45 min on ice. After washing, the cells were incubated with mFITC-conjugated anti-rat IgG2b (RG7/11.1, BD Biosciences) or anti-rat IgG2a (RG7/1.30, BD Biosciences) as the second antibody for non-conjugated anti-mouse ST2 mAbs for 45 min on ice. The expression of ST2 on 7-amino actinomycin D-negative FcεRIα$^+$ c-Kit$^+$ BMCMCs was

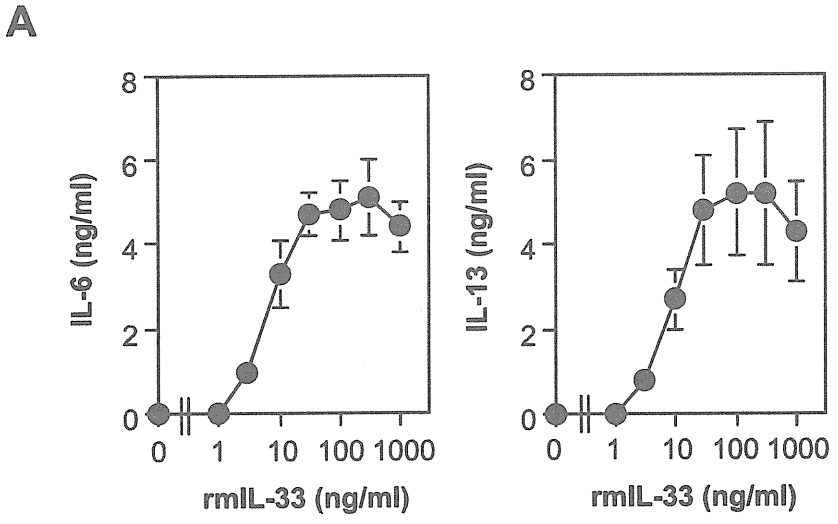
A
IL-6 (ng/ml)
IL-13 (ng/ml)
rmIL-33 (ng/ml)
rmIL-33 (ng/ml)
0
2
4
6
8
0
1
10
100
1000

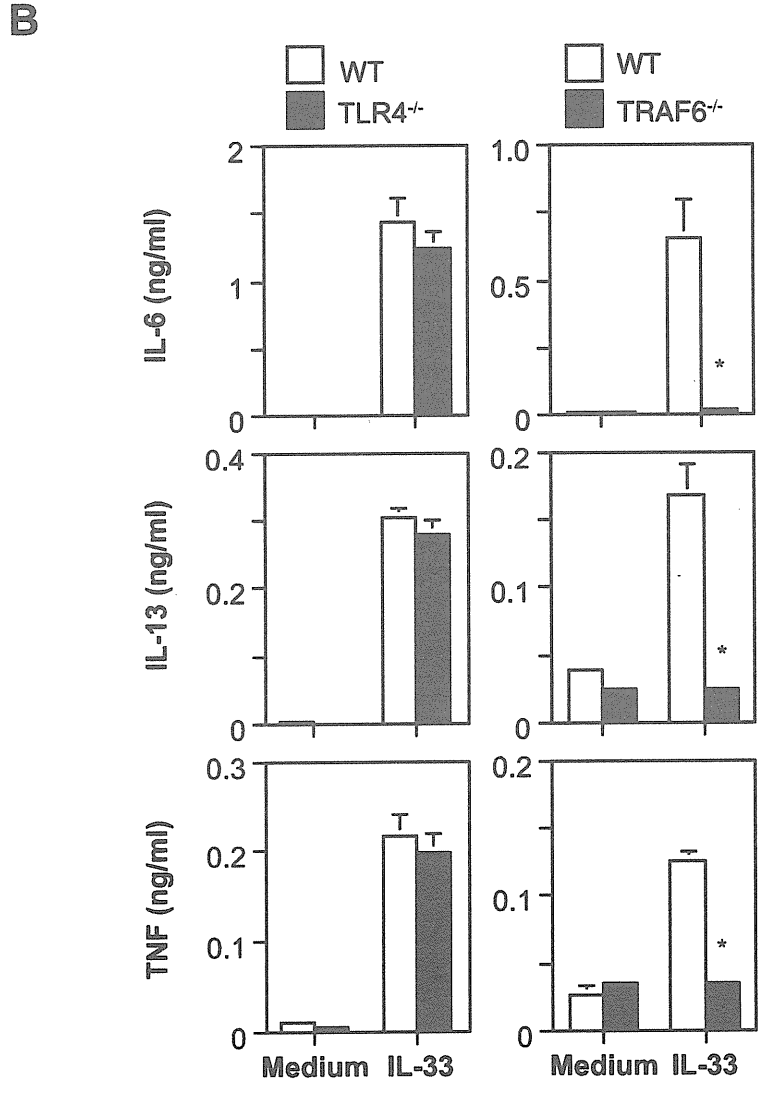
B
WT
TLR4-/-
WT
TRAF6-/-
IL-6 (ng/ml)
IL-13 (ng/ml)
TNF (ng/ml)
Medium
IL-33
Medium
IL-33
*
*
*

Figure 1. IL-33 induces TRAF6-dependent cytokine production by mast cells. BMCMCs obtained from B6J-WT mice (A) and B6J-WT and -TLR4$^{-/-}$ mice (B; left panels) and FLCMCs obtained from B6J-WT and -TRAF6$^{-/-}$ mice (B; right panels) were cultured in the presence of various concentration of rmIL-33 (A) or in the presence and absence of 100 ng/ml rmIL-33 for 6 h (for TNF measurement) and 24 h (for IL-6 and IL-13 measurement). The levels of IL-6, IL-13 and/or TNF in the culture supernatants were determined by ELISA. Data show the mean + SD (n = 3). *p<0.05 vs. WT.
doi:10.1371/journal.pone.0018404.g001

analyzed on a FACSCalibur flow cytometer (Becton Dickinson) using CellQuest software (Becton Dickinson).

Cell survival

TGC-induced peritoneal macrophages (1×10^6 cells/ml for FACS analysis and 2.5×10^5 cells/ml for lactate dehydrogenase [LDH] release assay, respectively) were cultured in the presence and absence of 100 ng/ml LPS for 0–48 h. Cell viability was assessed using a MEBCYTO-Apoptosis kit (MBL) or LDH assay kit (CytoTox 96; Promega) as described previously [44].

Cytokine ELISA

The levels of IL-6, IL-13 and TNF in culture supernatants were measured with mouse IL-6, IL-13 and TNF ELISA sets (eBioscience).

ELISPOT

The number of IL-33-secreting cells by ELISPOT assay was performed as described elsewhere [44]. Breifly, MultiScreen-IP plates (MAIPS4510; Millipore) were coated with anti-mouse IL-33 polyclonal Ab (R&D Systems; 2 μg/ml in PBS) as a capture Ab at 4°C overnight. After blocking with PBS containing 10% FCS, TGC-induced peritoneal macrophages (2×10^4/200 μl) were cultured in the presence or absence of 100 mg/ml LPS or 0.1 μg/ml PMA plus 1 μg/ml ionomycin at 37°C for 24 h or 48 h. After washing the wells, biotinylated anti-mouse/human IL-33 mAb (Nessy-1; Alexis Biochemicals, 400 ng/ml in PBS containing 10% FCS) as a detection Ab was applied and incubated at r.t. for 1 h. Then, after washing the wells, HRP-conjugated streptavidin (BD Biosciences) was added to the wells at r.t. for 1 h. AEC (Sigma) were used as substrates. Positive spots on Ab-coated plates were analyzed with NIH Image software.

Statistics

An unpaired Student's *t*-test, 2-tailed, was used for statistical evaluation of the results.

Results

Effects of anti-ST2 mAbs on cytokine production by BMCMCs

Several mAbs against mouse ST2, i.e., clones DJ8 [49,50], 3E10 [40], 245707 and 245714, have been generated to study the role(s) of ST2 in immune responses. It was recently demonstrated *in vitro* that IL-33-mediated cytokine production by macrophages was inhibited by addition of DJ8 [43], suggesting that DJ8 acts as a neutralizing Ab for IL-33 bioactivity. The crosslinking of ST2 by 3E10 enhanced Th2 cytokine production by Th2 cells *in vitro* [36], while the administration of 3E10 in mice resulted in the suppression of Th2 cell/cytokine-mediated allergic or viral airway inflammation [38,40,51] without depletion of ST2-expressing cells [37]. However, the effects of the other mAbs on IL-33-mediated immune cell activation remain unknown.

Recombinant mouse IL-33 (rmIL-33) can induce cytokine secretion by mouse bone marrow cell-derived cultured mast cells (BMCMCs) (Fig. 1A) dependent on MyD88, which is an essential adapter molecule for signal transduction of the TLR/IL-1R (TIR) superfamily [7]. As in the case of MyD88$^{-/-}$ BMCMCs [7] and ST2$^{-/-}$ BMCMCs (data not shown), IL-6, IL-13 and TNF production by FLCMCs deficient in TRAF6, which is a downstream molecule of MyD88, was impaired by rmIL-33 (derived from *E. coli*) (Fig. 1B). On the other hand, rmIL-33-mediated secretion of these cytokines was observed to be comparable in wild-type (WT) and TLR4$^{-/-}$ BMCMCs (Fig. 1), indicating that the biological activity of rmIL-33 was not influenced by contamination with endotoxin.

We next examined the effects of the anti-mouse ST2 mAbs on cytokine production by BMCMCs after IL-33 stimulation. Cytokine secretion by BMCMCs in response to 3–30 or 100 ng/mL rmIL-33 was profoundly or partially (nearly half maximum) inhibited in the presence of 40 μg/mL anti-ST2 mAb (DJ8), respectively (Fig. 2A). Therefore, we used 30 or 100 ng/mL rmIL-33 in the other neutralization studies. IL-33-mediated IL-6 and IL-13 production by WT BMCMCs was inhibited by addition of 245707 as well as DJ8, but not 3E10 or 245714 (Fig. 2B). Like rIL-33, it has been reported that crosslinking of ST2 by 3E10 promoted cytokine secretion by Th2 cells *in vitro* as an agonistic Ab [36]. On the other hand, 3E10 alone could not enhance IL-6 or IL-13 production by WT BMCMCs (Fig. 2B), although 3E10 as well as DJ8 and 245707, but not 245714, bound to ST2 on the cell surface of BMCMCs (Fig. 2C). We also found that crosslinking of ST2 by 3E10 and anti-rat IgG did not induce IL-6 or TNF production by BMCMCs (data not shown). These observations suggest that DJ8 and 245707, but not 3E10 or 245714, have neutralizing activity for IL-33-mediated mast cell activation, at least *in vitro*. Moreover, these observations indicate that the effect of 3E10 differs between Th2 cells [36] and mast cells.

Effects of anti-IL-33 mAb on cytokine production by BMCMCs

It was shown that ST2-expressing cells were depleted by anti-ST2 polyclonal Ab *in vitro* [52]. Therefore, anti-IL-33 Ab(s) rather than anti-ST2 Ab(s) would be useful for elucidating the role(s) of the IL-33-ST2 pathway *in vitro* and *in vivo*. Accordingly, we next examined the effects of anti-IL-33 mAbs (Nessy-1 and 518017) and polyclonal Ab (AF3626) on cytokine production by BMCMCs in response to rmIL-33. Nessy-1, but not 518017 or AF3626, inhibited IL-33-mediated IL-13 production by BMCMCs (Fig. 3A). However, the inhibitory effect of Nessy-1 was weak in comparison with that of the DJ8 anti-ST2 mAb, as shown in Figure 2A. Therefore, we newly generated anti-IL-33 mAbs (which were confirmed by western blot analysis to recognize rmIL-33; data not shown) and investigated their effects on IL-33-mediated cytokine production by BMCMCs. Ten (1D2, 1F11, 2A2, 2E6, 2C7, 4A3, 4D4, 4G4, 5F1 and 5D11) of 100 tested anti-IL-33 mAbs were able to inhibit IL-33-mediated IL-13 production (Fig. 3B). Like DJ8 (Fig. 2A), some of those mAbs (i.e., 2A2, 2E6 and so on) strongly inhibited IL-33 activity (Fig. 3B).

Effects of anti-IL-33 mAbs on cytokine production by TGC-induced macrophages and BMCMCs

It was recently reported that recombinant IL-33 enhanced LPS-mediated cytokine production by macrophages [43]. Consistent with this, we found that IL-33 augmented IL-6 production by

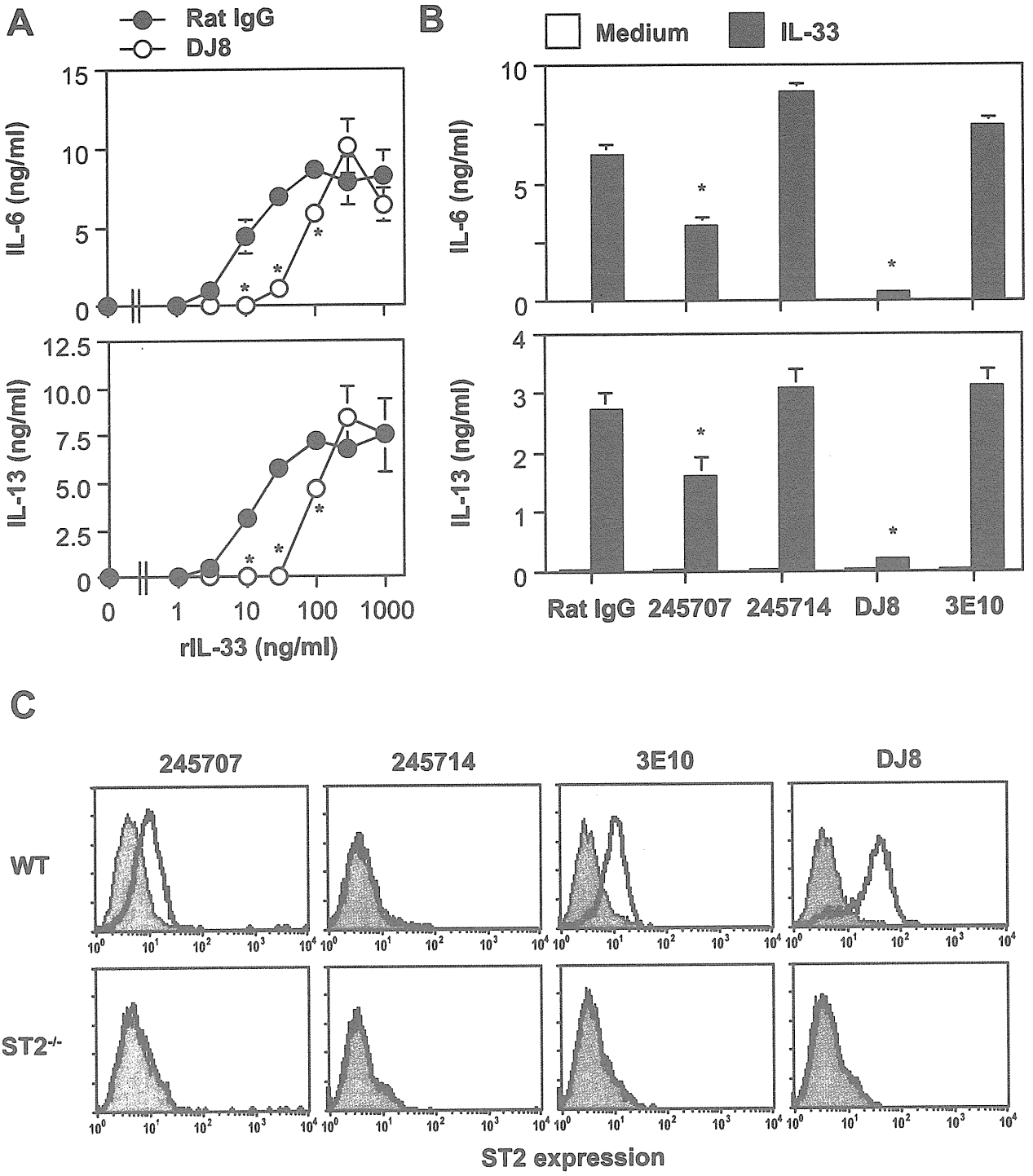

Figure 2. Effects of anti-ST2 mAbs on cytokine production by IL-33-stimulated BMCMCs. B6J-WT BMCMCs were stimulated with 0–1,000 ng/ml (A) or 100 ng/ml (B) rmIL-33 in the presence of 40 μg/ml of several anti-ST2 mAbs or isotype control rat IgG for 24 h. The levels of IL-6 and IL-13 in the culture supernatants were determined by ELISA. Data show the mean + SEM (n = 3). *$p<0.05$ vs. rat IgG+IL-33. The expression of ST2 on the cell surface of BALB-WT and ST2$^{-/-}$ BMCMCs was determined using several distinct anti-ST2 mAb clones. Representative data by flow cytometry are shown (C). Shaded area indicates isotype-matched control IgG staining, and bold line indicates anti-ST2 mAb staining.
doi:10.1371/journal.pone.0018404.g002

TGC-induced peritoneal macrophages in response to LPS (Fig. 4A). We reported that TGC-induced peritoneal macrophages produced IL-33 in response to LPS [44]. In addition, it is thought that IL-33 is released by necrotic cells after stimulation [53,54]. The proportion of annexin V-negative and propidium iodide (PI)-positive necrotic macrophages, the levels of LDH release in the

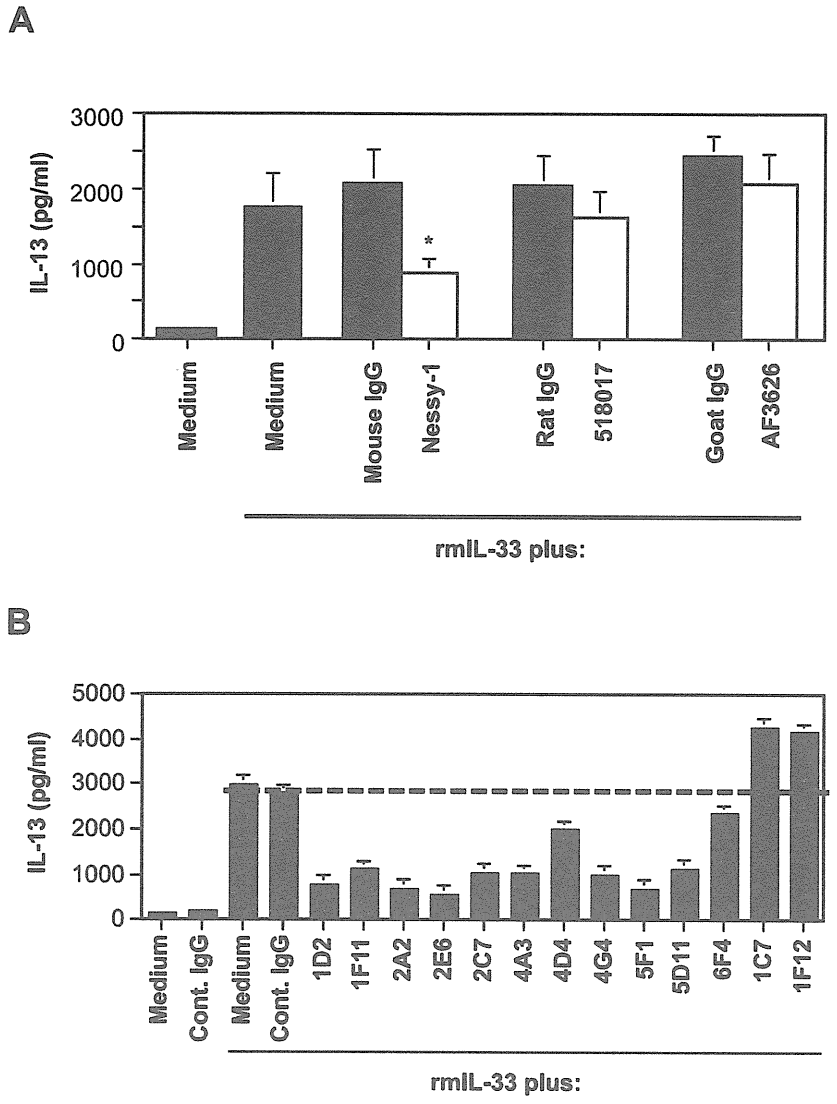

Figure 3. Effects of anti-IL-33 Abs on cytokine production by IL-33-stimulated BMCMCs. B6J-WT BMCMCs were stimulated with 30-ng/ml rmIL-33 in the presence and absence of commercially available anti-IL-33 Abs (A), our newly generated anti-IL-33 mAbs (B) or control IgG (A, B) for 24 h. The levels of IL-13 in the culture supernatants were determined by ELISA. Data show the mean + SEM (n = 3). *$p<0.05$ vs. control IgG+IL-33.
doi:10.1371/journal.pone.0018404.g003

culture supernatants and the number of IL-33-secreting macrophages were significantly increased at 48 h after LPS stimulation (Fig. 4B–D). Consistent with previous reports [44], we could not detect IL-33 proteins in the culture supernatants and cell lysates by ELISA and western blot analysis, respectively (data not shown). These observations suggest that necrotic macrophage-derived IL-33 may paracrinely promote cytokine production by viable macrophages after LPS stimulation. In support of this, IL-6 production by IL-33$^{-/-}$ macrophages was reduced in comparison with WT macrophages at 24 and 48 h after LPS stimulation (Fig. 4E). To more fully elucidate this, we examined the effects of endogenous IL-33 on cytokine production by LPS-stimulated TGC-induced macrophages in the presence of anti-ST2 mAbs and anti-IL-33 mAbs. The LPS-mediated IL-6 production by TGC-induced macrophages was inhibited by addition of anti-ST2 mAbs DJ8 and 245707, but not 3E10 or 245714 at 48 h, but not 24 h, after LPS stimulation (Fig. 5A). These responses by TGC-induced macrophages were also inhibited by addition of anti-IL-33 mAbs 2C7 and 1F11, but not other mAbs including 5D11, 1D2, 2A2 and 2E6, at 48 h, but not 24 h, after LPS stimulation (Fig. 5B and data not shown). We previously demonstrated that IL-33 mRNA expression was increased in BMCMCs after stimulation with highly cytokinergic IgE [55], FcεRI-crosslinking by IgE and antigens, and PMA+ionomycin, but not LPS [44]. However, the expression level of IL-33 protein by BMCMCs was less than that by TGC-induced macrophages after stimulation [44]. In accordance with this, IL-13 production by BMCMCs was not influenced by addition of any of the anti-IL-33 mAbs at 48 h after IgE stimulation (anti-DNP IgE; SPE-7) (Fig. 5C). These observations suggest that macrophages, rather than mast cells, are potential producers of IL-33, and that macrophage-derived IL-33 can activate macrophages in a paracrine manner after LPS stimulation.

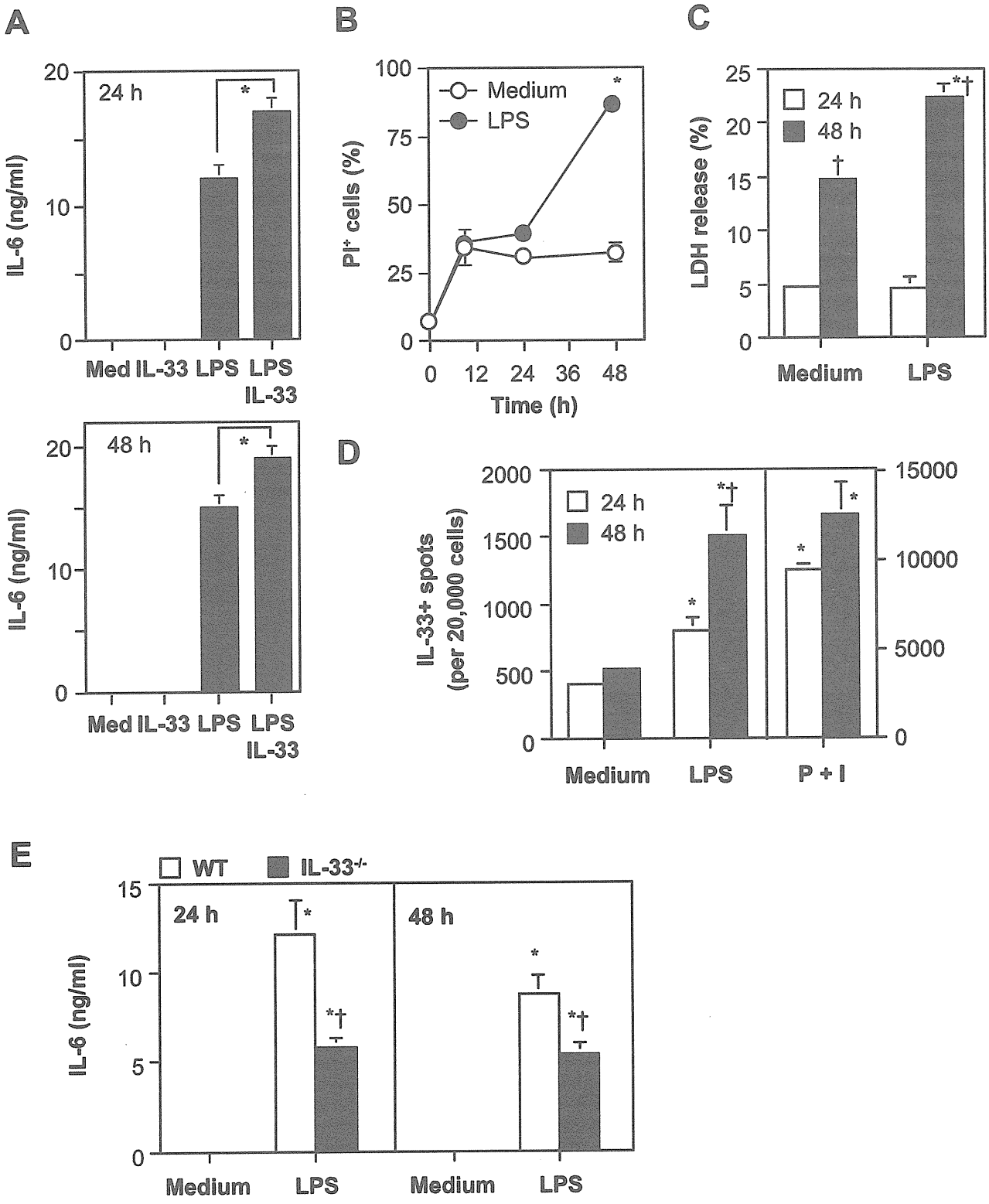

Figure 4. IL-33 enhances LPS-mediated cytokine production by macrophages. TGC-induced peritoneal macrophages derived from B6J-WT mice (A–D) and B6N-WT and -IL-33$^{-/-}$ mice (E) were cultured in the presence and absence of 100 ng/ml LPS, with and without 100 ng/ml IL-33, for 9, 24 and/or 48 h. (A, E) The levels of IL-6 in the culture supernatants by ELISA. (B) The percentage of PI-positive cells by flow cytometry. (C) LDH levels in the culture supernatants. (D) The number of IL-33-secreting cells by ELISPOT. Data show the mean +/± SEM (n = 3 [A] or 4 [B–E]). *$p<0.05$ vs. the indicated group (A) or Medium (B–E), and $^{\dagger}p<0.05$ vs. 24 h (C, D) or WT (E). P+I = PMA+ionomycin.
doi:10.1371/journal.pone.0018404.g004

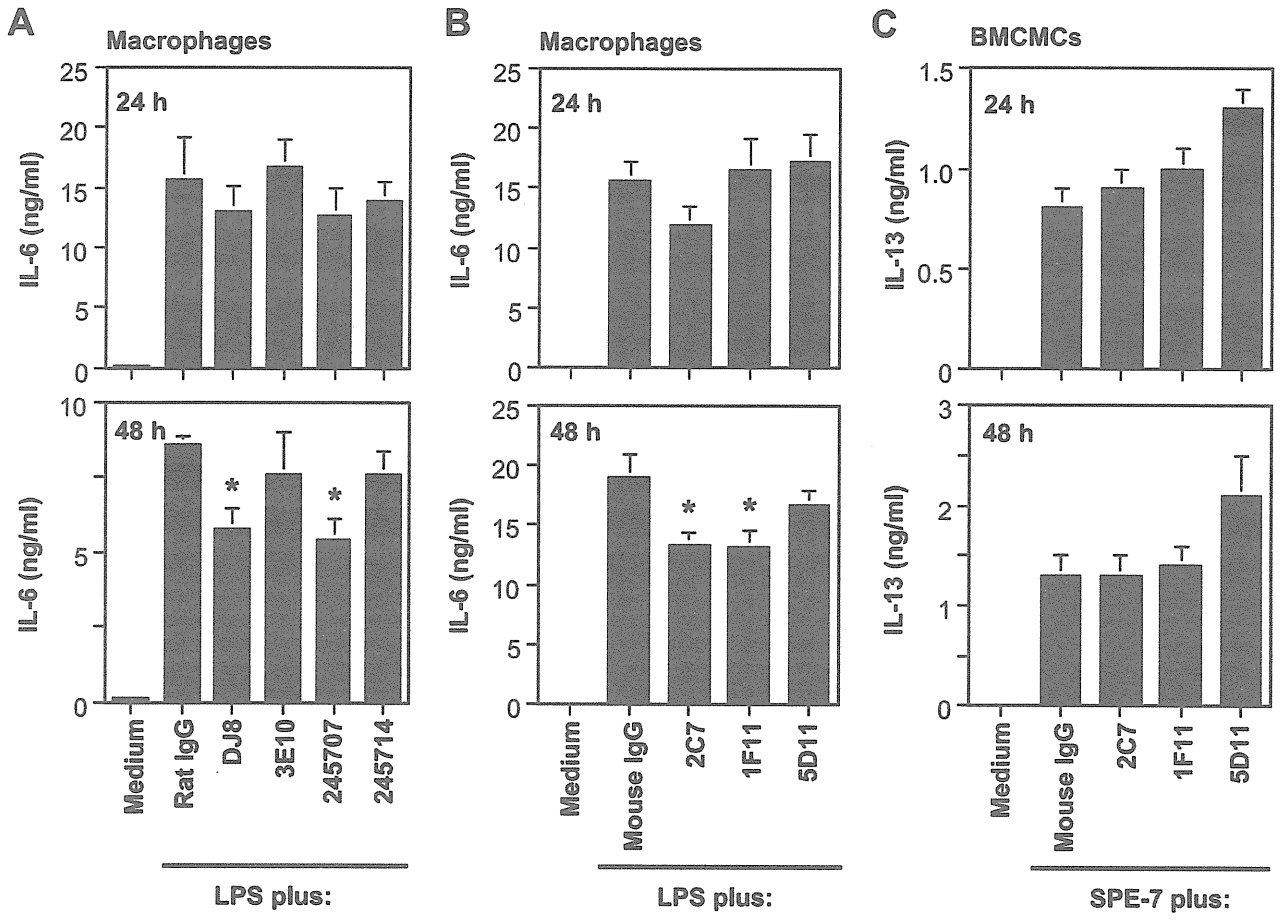

Figure 5. Inhibitory effects of anti-IL-33 mAbs on LPS-mediated macrophage activation by paracrine IL-33 stimulation. (A, B) TGC-induced peritoneal macrophages derived from B6J-WT mice were cultured in the presence of 100 ng/ml LPS, with and without 40 μg/ml of several anti-ST2 mAbs (A), several anti-IL-33 mAbs (B) or control IgG (A, B) for 24 and 48 h. (C) B6J-WT BMCMCs were cultured in the presence of 1 μg/ml anti-DNP IgE (SPE-7), with and without 40 μg/ml of several anti-IL-33 mAbs or control IgG for 24 and 48 h. The levels of IL-6 or IL-13 in the culture supernatants were measured by ELISA. Data show the mean + SEM ([A] n = 7, [B] n = 8 [C] n = 4). *$p<0.05$ vs. Rat IgG (A) or Mouse IgG (B).
doi:10.1371/journal.pone.0018404.g005

Discussion

Like ST2$^{-/-}$ mice [56] and mice treated with a soluble ST2-Fc fusion protein [57], mice treated with a certain anti-ST2 mAb (generated by Amgen) showed attenuated development of collagen-induced arthritis [58]. Since that ST2 mAb (Amgen) inhibited IL-33-mediated immune responses *in vitro* and *in vivo*, it is considered to act as a blocking Ab for binding of IL-33 to ST2. Conversely, mice treated with an anti-ST2 polyclonal Ab showed aggravated development of collagen-induced arthritis [52]. Since that polyclonal Ab lysed ST2-expressing cells *in vitro*, its *in vivo* administration may have depleted certain ST2-expressing regulatory cells such as Tr1 cells [59] as well as ST2-expressing effector cells such as mast cells [56], thereby causing aggravation, rather than attenuation, of the arthritis. However, the precise activities (i.e., depletion, agonism, blocking, etc.) of the other ST2 Abs were poorly characterized in the previous studies, because many of which were performed before the identification of IL-33.

It is well known that the biological activities of the IL-1 family of cytokines are elaborately regulated by decoy/soluble receptors, binding proteins and/or receptor antagonists [60,61]. For example, the activities of IL-1α and IL-1β are mediated by IL-1R (IL-1R1 and IL-1RAcP), but blocked by IL-1R2, the soluble form IL-1Rs and IL-1 receptor antagonist (IL-1Ra) [60,61]. The activities of IL-18 are mediated by IL-18R, but inhibited by IL-18-binding protein [60,61]. On the other hand, inconsistent results were reported between a ligand- and its receptor-deficient mice even on the same genetic background. For example, experimental autoimmune encephalomyelitis developed normally in IL-18$^{-/-}$ mice, but not in IL-18Rα$^{-/-}$ mice [62]. These observations suggest involvement of another ligand(s) besides IL-18, i.e., IL-1F7 [63], in the development of the disease. Moreover, IL-1F10, in addition to IL-1α, IL-1β and IL-1Ra, also can bind to IL-1R1, although its binding affinity is low compared with IL-1β and IL-1Ra [64]. Therefore, like IL-18Rα and IL-1R1, ST2 may be a component of receptors for another ligand(s) besides IL-33. As another possibility, IL-33 may bind to other receptors besides ST2, SIGIRR/Tir8 [65] and c-Kit [66]. Thus, it was surmised that, for elucidation of the precise roles of IL-33 *in vivo* and *in vitro*, it would be more advantageous to use neutralizing Abs for IL-33 rather than for ST2. Therefore, in the present study, we newly generated anti-IL-33 mAbs and characterized their functions as well as the functions of anti-ST2 Abs.

We and the others have shown that macrophages can release IL-33 after LPS stimulation [44], and IL-33 can enhance LPS-mediated TNF and IL-6 production by macrophages (Fig. 4A)

[43]. We also found that IL-33$^{-/-}$ macrophages showed reduced IL-6 production in response to LPS (Fig. 4C). Likewise, LPS-mediated IL-6 production by macrophages was inhibited by treatment with anti-IL-33 mAbs (2C7 and 1F11, but not other mAbs) (Fig. 5B and data not shown), a soluble ST2-Fc fusion protein [15] or anti-ST2 mAbs (DJ8 and 245707, but not 3E10 and 245714) (Fig. 5A). It was reported that IL-1, IL-6, IL-12 and TNF production by macrophages from ST2$^{-/-}$ mice on the BALB/c background was increased [16] or comparable [43] with those from wild-type mice at 12, 24 or 48 h after LPS stimulation. The apparent discrepancy between ST2$^{-/-}$ macrophages and IL-33$^{-/-}$/anti-ST2 mAb-treated/soluble ST2-Fc fusion protein-treated macrophages may be accounted for as described elsewhere [4]. Nonetheless, these observations (except the study using ST2$^{-/-}$ macrophages [16]) suggest that macrophages produce IL-33 in response to LPS, and that that IL-33 then additively promotes LPS-mediated macrophage activation.

The inhibitory levels of cytokine production by macrophages treated with anti-IL-33 neutralizing Ab was lesser than those by IL-33$^{-/-}$ macrophages after LPS stimulation. It is considered that IL-33 has dual roles as a cytokine and a nuclear factor [67,68,69]. The function of both secreted and nuclear IL-33 was abrogated in IL-33-deficient cells. On the other hand, the neutralizing antibody for IL-33 and/or ST2 can inhibit the effect of secreted IL-33, but not that of nuclear IL-33. Thus, the difference between anti-IL-33 neutralizing antibody-treated and IL-33-deficient macrophages may be due to the potential role of IL-33 in the nucleus.

Anti-IL-33 mAb 5D11 inhibited recombinant IL-33$_{109-266}$-dependent IL-13 production by BMCMCs (Fig. 3B). Conversely, it did not inhibit the activity of endogenous IL-33 (probably full-length IL-33) in LPS-mediated IL-6 production by macrophages (Fig. 5B). Like anti-IL-33 mAb Nessy-1, our anti-IL-33 mAbs were generated against IL-33$_{109-266}$, not full-length IL-33, and it seemed that some of them including 1D2, 2A2, and 2E6 could not inhibit the activities of full-length IL-33 even though they neutralized recombinant IL-33$_{109-266}$ (Fig. 3B and data not shown).

In conclusion, our findings suggest that IL-33-neutralizing mAbs, which we newly generated, will be useful tools for the understanding the pathophysiological function(s) of IL-33 *in vitro* and presumably *in vivo*. They also have potential for aiding in the development of new therapeutics for certain IL-33-mediated disorders.

Acknowledgments

We thank Drs. Tsuneyasu Kaisyo and (RIKEN, Japan) and Andrew N.J. McKenzie (MRC, Cambridge, UK) for providing B6J-TLR4$^{-/-}$ mice and BALB-ST2$^{-/-}$ mice, and Michiko Yamada, Hiromi Wakita, Shuhei Fukuda and Noriko Hashimoto for their excellent technical assistance.

Author Contributions

Analyzed the data: TO K. Oboki KA HM NK. Contributed reagents/materials/analysis tools: M. Iikura TA JI KM KS MA K. Okumura TK HS. Wrote the paper: TO K. Oboki SN. Designed the study: TO K. Oboki SN. Performed the research: TO K. Oboki KA HM NK. Generation of anti-IL-33 mAbs: ST M. Ikeda.

References

1. Schmitz J, Owyang A, Oldham E, Song Y, Murphy E, et al. (2005) IL-33, an interleukin-1-like cytokine that signals via the IL-1 receptor-related protein ST2 and induces T helper type 2-associated cytokines. Immunity 23: 479–490.
2. Smith DE (2010) IL-33: a tissue derived cytokine pathway involved in allergic inflammation and asthma. Clin Exp Allergy 40: 200–208.
3. Liew FY, Pitman NI, McInnes IB (2010) Disease-associated functions of IL-33: the new kid in the IL-1 family. Nat Rev Immunol 10: 103–110.
4. Oboki K, Ohno T, Kajiwara N, Saito H, Nakae S (2010) IL-33 and IL-33 receptors in host defense and diseases. Allergol Int 59: 143–160.
5. Chackerian AA, Oldham ER, Murphy EE, Schmitz J, Pflanz S, et al. (2007) IL-1 receptor accessory protein and ST2 comprise the IL-33 receptor complex. J Immunol 179: 2551–2555.
6. Cherry WB, Yoon J, Bartemes KR, Iijima K, Kita H (2008) A novel IL-1 family cytokine, IL-33, potently activates human eosinophils. J Allergy Clin Immunol 121: 1484–1490.
7. Ho LH, Ohno T, Oboki K, Kajiwara N, Suto H, et al. (2007) IL-33 induces IL-13 production by mouse mast cells independently of IgE-FcepsilonRI signals. J Leukoc Biol 82: 1481–1490.
8. Moulin D, Donze O, Talabot-Ayer D, Mezin F, Palmer G, et al. (2007) Interleukin (IL)-33 induces the release of pro-inflammatory mediators by mast cells. Cytokine 40: 216–225.
9. Iikura M, Suto H, Kajiwara N, Oboki K, Ohno T, et al. (2007) IL-33 can promote survival, adhesion and cytokine production in human mast cells. Lab Invest 87: 971–978.
10. Allakhverdi Z, Smith DE, Comeau MR, Delespesse G (2007) The ST2 ligand IL-33 potently activates and drives maturation of human mast cells. J Immunol 179: 2051–2054.
11. Ali S, Huber M, Kollewe C, Bischoff SC, Falk W, et al. (2007) IL-1 receptor accessory protein is essential for IL-33-induced activation of T lymphocytes and mast cells. Proc Natl Acad Sci U S A 104: 18660–18665.
12. Suzukawa M, Iikura M, Koketsu R, Nagase H, Tamura C, et al. (2008) An IL-1 cytokine member, IL-33, induces human basophil activation via its ST2 receptor. J Immunol 181: 5981–5989.
13. Pecaric-Petkovic T, Didichenko SA, Kaempfer S, Spiegl N, Dahinden CA (2009) Human basophils and eosinophils are the direct target leukocytes of the novel IL-1 family member IL-33. Blood 113: 1526–1534.
14. Kondo Y, Yoshimoto T, Yasuda K, Futatsugi-Yumikura S, Morimoto M, et al. (2008) Administration of IL-33 induces airway hyperresponsiveness and goblet cell hyperplasia in the lungs in the absence of adaptive immune system. Int Immunol 20: 791–800.
15. Sweet MJ, Leung BP, Kang D, Sogaard M, Schulz K, et al. (2001) A novel pathway regulating lipopolysaccharide-induced shock by ST2/T1 via inhibition of Toll-like receptor 4 expression. J Immunol 166: 6633–6639.
16. Brint EK, Xu D, Liu H, Dunne A, McKenzie AN, et al. (2004) ST2 is an inhibitor of interleukin 1 receptor and Toll-like receptor 4 signaling and maintains endotoxin tolerance. Nat Immunol 5: 373–379.
17. Allakhverdi Z, Comeau MR, Smith DE, Toy D, Endam LM, et al. (2009) CD34^{+} hemopoietic progenitor cells are potent effectors of allergic inflammation. J Allergy Clin Immunol 123: 472–478.
18. Moro K, Yamada T, Tanabe M, Takeuchi T, Ikawa T, et al. (2010) Innate production of T(H)2 cytokines by adipose tissue-associated c-Kit^{+}Sca-1^{+} lymphoid cells. Nature 463: 540–544.
19. Neill DR, Wong SH, Bellosi A, Flynn RJ, Daly M, et al. (2010) Nuocytes represent a new innate effector leukocyte that mediates type-2 immunity. Nature 464: 1367–1370.
20. Gudbjartsson DF, Bjornsdottir US, Halapi E, Helgadottir A, Sulem P, et al. (2009) Sequence variants affecting eosinophil numbers associate with asthma and myocardial infarction. Nat Genet 41: 342–347.
21. Reijmerink NE, Postma DS, Bruinenberg M, Nolte IM, Meyers DA, et al. (2008) Association of IL1RL1, IL18R1, and IL18RAP gene cluster polymorphisms with asthma and atopy. J Allergy Clin Immunol 122: 651–654 e658.
22. Ali M, Zhang G, Thomas WR, McLean CJ, Bizzintino JA, et al. (2009) Investigations into the role of ST2 in acute asthma in children. Tissue Antigens 73: 206–212.
23. Shimizu M, Matsuda A, Yanagisawa K, Hirota T, Akahoshi M, et al. (2005) Functional SNPs in the distal promoter of the ST2 gene are associated with atopic dermatitis. Hum Mol Genet 14: 2919–2927.
24. Sakashita M, Yoshimoto T, Hirota T, Harada M, Okubo K, et al. (2008) Association of serum interleukin-33 level and the interleukin-33 genetic variant with Japanese cedar pollinosis. Clin Exp Allergy 38: 1875–1881.
25. Castano R, Bosse Y, Endam LM, Desrosiers M (2009) Evidence of association of interleukin-1 receptor-like 1 gene polymorphisms with chronic rhinosinusitis. Am J Rhinol Allergy 23: 377–384.
26. Smithgall MD, Comeau MR, Yoon BR, Kaufman D, Armitage R, et al. (2008) IL-33 amplifies both Th1- and Th2-type responses through its activity on human basophils, allergen-reactive Th2 cells, iNKT and NK cells. Int Immunol 20: 1019–1030.
27. Kurowska-Stolarska M, Stolarski B, Kewin P, Murphy G, Corrigan CJ, et al. (2009) IL-33 amplifies the polarization of alternatively activated macrophages that contribute to airway inflammation. J Immunol 183: 6469–6477.
28. Kuroiwa K, Li H, Tago K, Iwahana H, Yanagisawa K, et al. (2000) Construction of ELISA system to quantify human ST2 protein in sera of patients. Hybridoma 19: 151–159.
29. Oshikawa K, Kuroiwa K, Tago K, Iwahana H, Yanagisawa K, et al. (2001) Elevated soluble ST2 protein levels in sera of patients with asthma with an acute exacerbation. Am J Respir Crit Care Med 164: 277–281.